Appendix A

Thermodynamic Properties

A.1. Seawater Density

The density correlation for seawater is given by

$$\rho = 10^3 (A_1 F_1 + A_2 F_2 + A_3 F_3 + A_4 F_4) \quad (A.1)$$

where

$B = ((2)(X)/1000-150)/150$

$G_1 = 0.5$

$G_2 = B$

$G_3 = 2 B^2 - 1$

$A_1 = 4.032219 G_1 + 0.115313 G_2 + 3.26\text{x}10^{-4} G_3$

$A_2 = -0.108199 G_1 + 1.571\text{x}10^{-3} G_2 - 4.23\text{x}10^{-4} G_3$

$A_3 = -0.012247 G_1 + 1.74\text{x}10^{-3} G_2 - 9\text{x}10^{-6} G_3$

$A_4 = 6.92\text{x}10^{-4} G_1 - 8.7\text{x}10^{-5} G_2 - 5.3\text{x}10^{-5} G_3$

$A = ((2)(T) - 200)/160$

$F_1 = 0.5$, $F_2 = A$, $F_3 = 2 A^2 - 1$, $F_4 = 4 A^3 - 3 A$

In the above equations ρ is the seawater density in kg/m^3, X is the seawater salinity in ppm, and T is the seawater temperature in °C. This correlation is valid over the following ranges: $0 \leq X \leq 160000$ ppm and $10 \leq T \leq 180$ °C. Variations in the seawater density as a function of temperature and salinity are given in Table A.1 and Fig. A.1.

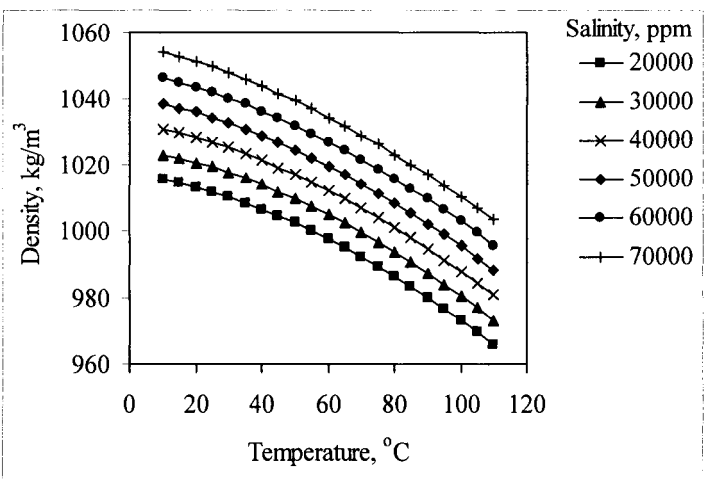

Figure A.1: Variation in density of seawater as a function of temperature and salinity.

Table A.1: Variation in seawater density (kg/m^3) as a function of temperature (°C) and salinity (ppm)

	Salinity ppm						
T (°C)	10000	20000	30000	40000	50000	60000	70000
10	1008	1015	1023	1031	1038	1046	1054
15	1007	1014	1022	1030	1037	1045	1053
20	1006	1013	1021	1028	1036	1044	1051
25	1004	1012	1019	1027	1034	1042	1050
30	1003	1010	1018	1025	1033	1040	1048
35	1001	1008	1016	1023	1031	1038	1046
40	999	1007	1014	1021	1029	1036	1044
45	997	1004	1012	1019	1027	1034	1042
50	995	1002	1010	1017	1024	1032	1039
55	993	999.9	1007	1015	1022	1029	1037
60	990	997.5	1005	1012	1020	1027	1034
65	988	994.9	1002	1010	1017	1024	1032
70	985	992.2	999.5	1007	1014	1022	1029
75	982	989.3	996.6	1004	1011	1019	1026
80	979	986.3	993.7	1001	1008	1016	1023
85	976	983.2	990.6	997.9	1005	1013	1020
90	973	980	987.4	994.7	1002	1010	1017
95	969	976.7	984	991.4	998.8	1006	1014
100	966	973.2	980.6	988	995.4	1003	1010
105	962	969.6	977	984.4	991.9	999.3	1007
110	958	965.9	973.3	980.8	988.3	995.7	1003

A.2. Seawater Specific Heat at Constant Pressure

The seawater specific heat at constant pressure is given by the following correlation

$$C_p = (A + BT + CT^2 + DT^3)x10^{-3} \quad (A.2)$$

The variables A, B, C and D are evaluated as a function of the water salinity as follows:

$$A = 4206.8 - 6.6197\ s + 1.2288x10^{-2}\ s^2$$

$$B = -1.1262 + 5.4178x10^{-2}\ s - 2.2719x10^{-4}\ s^2$$

$$C = 1.2026x10^{-2} - 5.3566x10^{-4}\ s + 1.8906x10^{-6}\ s^2$$

$$D = 6.8777x10^{-7} + 1.517x10^{-6}\ s - 4.4268x10^{-9}\ s^2$$

where Cp in kJ/kg °C, T in °C, and s is the water salinity in gm/kg. The above correlation is valid over salinity and temperature ranges of $20000 \leq X \leq 160000$ ppm and $20 \leq T \leq 180$ °C, respectively. Variations in the seawater specific heat as a function of temperature and salinity are given in Table A.2 and Fig. A.2.

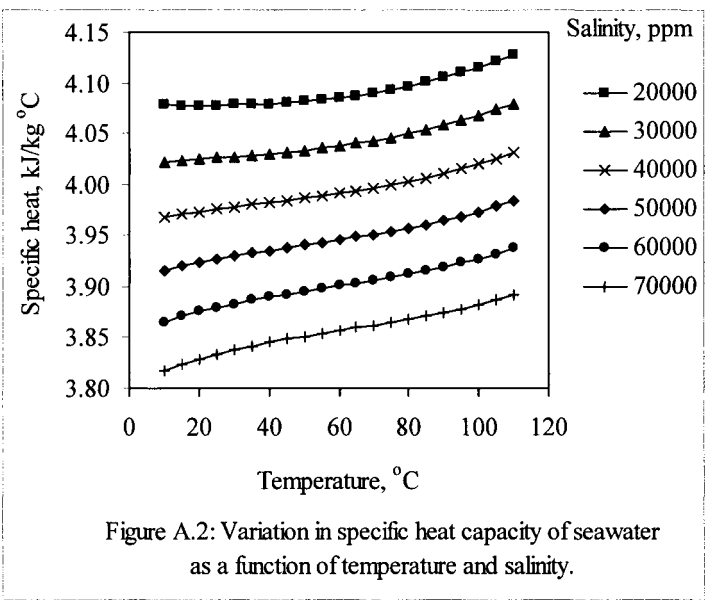

Figure A.2: Variation in specific heat capacity of seawater as a function of temperature and salinity.

Table A.2: Variation in seawater specific heat (kJ/kg °C) as a function of temperature (°C) and salinity (ppm)

	Salinity ppm						
T (°C)	10000	20000	30000	40000	50000	60000	70000
10	4.14	4.078	4.022	3.968	3.916	3.866	3.818
15	4.13	4.078	4.023	3.971	3.92	3.871	3.824
20	4.13	4.078	4.025	3.973	3.923	3.875	3.829
25	4.13	4.078	4.026	3.976	3.927	3.879	3.834
30	4.13	4.078	4.027	3.978	3.93	3.883	3.838
35	4.13	4.078	4.029	3.98	3.933	3.887	3.842
40	4.13	4.079	4.03	3.982	3.935	3.89	3.845
45	4.13	4.08	4.032	3.984	3.938	3.893	3.849
50	4.13	4.082	4.033	3.986	3.94	3.895	3.851
55	4.13	4.083	4.035	3.989	3.943	3.898	3.854
60	4.13	4.085	4.038	3.991	3.945	3.901	3.857
65	4.14	4.087	4.04	3.994	3.948	3.903	3.86
70	4.14	4.09	4.043	3.997	3.951	3.906	3.862
75	4.14	4.093	4.046	4	3.954	3.909	3.865
80	4.15	4.097	4.05	4.003	3.957	3.912	3.868
85	4.15	4.101	4.053	4.007	3.961	3.915	3.871
90	4.15	4.105	4.058	4.011	3.964	3.919	3.874
95	4.16	4.11	4.062	4.015	3.969	3.923	3.878
100	4.17	4.116	4.068	4.02	3.973	3.927	3.882
105	4.17	4.122	4.073	4.025	3.978	3.932	3.887
110	4.18	4.129	4.08	4.031	3.984	3.937	3.892

A.3. Seawater Dynamic Viscosity

The correlation for the dynamic viscosity of seawater is given by

$$\mu = (\mu_W)\,(\mu_R) \times 10^{-3} \qquad \text{(A.3)}$$

with

$$\text{Ln}(\mu_W) = -3.79418 + 604.129/(139.18+T)$$

$$\mu_R = 1 + A\,s + B\,s^2$$

$$A = 1.474\text{x}10^{-3} + 1.5\text{x}10^{-5}\,T - 3.927\text{x}10^{-8}\,T^2$$

$$B = 1.0734\text{x}10^{-5} - 8.5\text{x}10^{-8}\,T + 2.23\text{x}10^{-10}\,T^2$$

where μ in kg/m s, T in °C, and s in gm/kg. The above correlation is valid over the following ranges $0 \leq s \leq 130$ gm/kg and $10 \leq T \leq 180$ °C. Variations in the seawater viscosity as a function of temperature and salinity are given in Table A.3 and Fig. A.3.

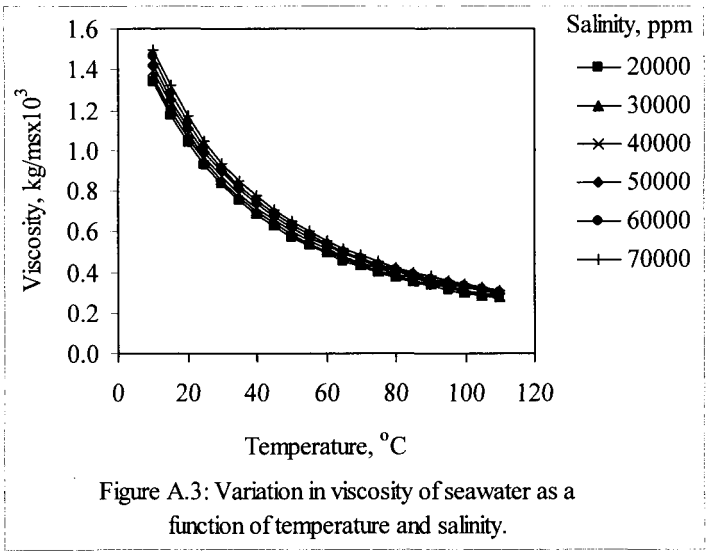

Figure A.3: Variation in viscosity of seawater as a function of temperature and salinity.

Table A.3: Variation in seawater viscosity (kg/m s) as a function of temperature (°C) and salinity (ppm)

	Salinity ppm						
T (°C)	10000	20000	30000	40000	50000	60000	70000
10	1.31	1.338	1.365	1.395	1.428	1.463	1.5
15	1.15	1.175	1.199	1.226	1.255	1.286	1.319
20	1.02	1.04	1.062	1.086	1.112	1.14	1.169
25	0.91	0.928	0.948	0.969	0.993	1.018	1.044
30	0.82	0.833	0.851	0.871	0.892	0.915	0.939
35	0.74	0.753	0.77	0.788	0.807	0.827	0.849
40	0.67	0.684	0.7	0.716	0.734	0.753	0.772
45	0.61	0.625	0.639	0.655	0.671	0.688	0.706
50	0.56	0.573	0.587	0.601	0.616	0.632	0.649
55	0.52	0.529	0.541	0.555	0.569	0.584	0.599
60	0.48	0.489	0.501	0.514	0.527	0.541	0.555
65	0.44	0.455	0.466	0.478	0.49	0.503	0.516
70	0.41	0.424	0.435	0.446	0.457	0.469	0.482
75	0.39	0.397	0.407	0.417	0.428	0.439	0.451
80	0.36	0.372	0.382	0.392	0.402	0.413	0.424
85	0.34	0.35	0.359	0.369	0.379	0.389	0.399
90	0.32	0.33	0.339	0.348	0.357	0.367	0.377
95	0.3	0.313	0.321	0.329	0.338	0.347	0.357
100	0.29	0.296	0.304	0.312	0.321	0.33	0.338
105	0.27	0.282	0.289	0.297	0.305	0.313	0.322
110	0.26	0.268	0.275	0.283	0.291	0.298	0.307

A.4. Seawater Thermal Conductivity

The seawater thermal conductivity is given by

$$\mathrm{Log}_{10}(k) = \mathrm{Log}_{10}(240 + A\,s) + 0.434\left(2.3 - \frac{343.5 + B\,s}{T + 273.15}\right)\left(1 - \frac{T + 273.15}{647.3 + C\,s}\right)^{1/3} \quad (A.4)$$

where k is the thermal conductivity in W/m °C, s is the salinity in gm/kg, T is the temperature in °C. The constants A, B, and C are equal to $2x10^{-4}$, $3.7x10^{-2}$, and $3x10^{-2}$, respectively. The above correlation valid over the following ranges, $0 \leq s \leq 160$ gm/kg and $20 \leq T \leq 180$ °C. Variations in the seawater thermal conductivity as a function of temperature and salinity are given in Table A.4 and Fig. A.4.

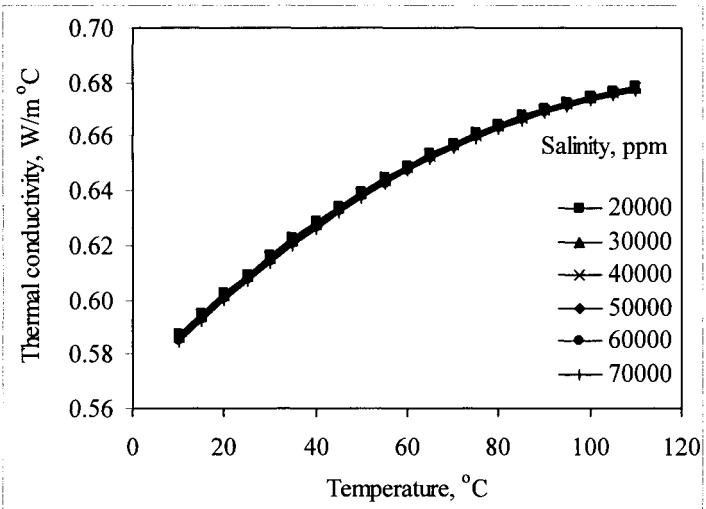

Figure A.4: Variation in thermal conductivity of seawater as a function of temperature and salinity.

Table A.4: Variation in seawater thermal conductivity (kW/m°C) as a function of temperature (°C) and salinity (gm/kg)

	Salinity (gm/kg)						
T (°C)	10	20	30	40	50	60	70
10	0.5877	0.5872	0.5866	0.586	0.5855	0.5849	0.5844
15	0.5955	0.595	0.5944	0.5939	0.5933	0.5928	0.5922
20	0.603	0.6024	0.6019	0.6013	0.6008	0.6003	0.5997
25	0.61	0.6095	0.609	0.6084	0.6079	0.6074	0.6068
30	0.6168	0.6162	0.6157	0.6152	0.6147	0.6141	0.6136
35	0.6231	0.6226	0.6221	0.6216	0.621	0.6205	0.62
40	0.6291	0.6286	0.6281	0.6276	0.6271	0.6266	0.6261
45	0.6347	0.6343	0.6338	0.6333	0.6328	0.6323	0.6318
50	0.6401	0.6396	0.6391	0.6386	0.6381	0.6377	0.6372
55	0.645	0.6446	0.6441	0.6436	0.6432	0.6427	0.6422
60	0.6497	0.6492	0.6488	0.6483	0.6478	0.6474	0.6469
65	0.654	0.6535	0.6531	0.6527	0.6522	0.6518	0.6513
70	0.658	0.6575	0.6571	0.6567	0.6563	0.6558	0.6554
75	0.6616	0.6612	0.6608	0.6604	0.66	0.6596	0.6591
80	0.665	0.6646	0.6642	0.6638	0.6634	0.663	0.6626
85	0.6681	0.6677	0.6673	0.6669	0.6665	0.6661	0.6657
90	0.6708	0.6704	0.6701	0.6697	0.6693	0.6689	0.6686
95	0.6733	0.6729	0.6725	0.6722	0.6718	0.6715	0.6711
100	0.6754	0.6751	0.6747	0.6744	0.674	0.6737	0.6733
105	0.6773	0.677	0.6766	0.6763	0.676	0.6756	0.6753
110	0.6789	0.6786	0.6783	0.6779	0.6776	0.6773	0.677

A.5. Enthalpy of Saturated Liquid Water

The correlation for enthalpy of saturated liquid water is given by

$$H = -0.033635409 + 4.207557011\,T - 6.200339\times10^{-4}\,T^2 + 4.459374\times10^{-6}\,T^3 \quad (A.5)$$

In the above equation, T is the saturation temperature in °C and H is the enthalpy in kJ/kg. Values for the calculated enthalpy over a temperature range of 5-200 °C are given in Table A.5. The table also includes values extracted from the steam tables. The percentage errors for the calculated versus the steam table values are less than 0.04%. Figure A.5 show variations in the calculated and the steam tables values for the liquid water enthalpy as a function of temperature.

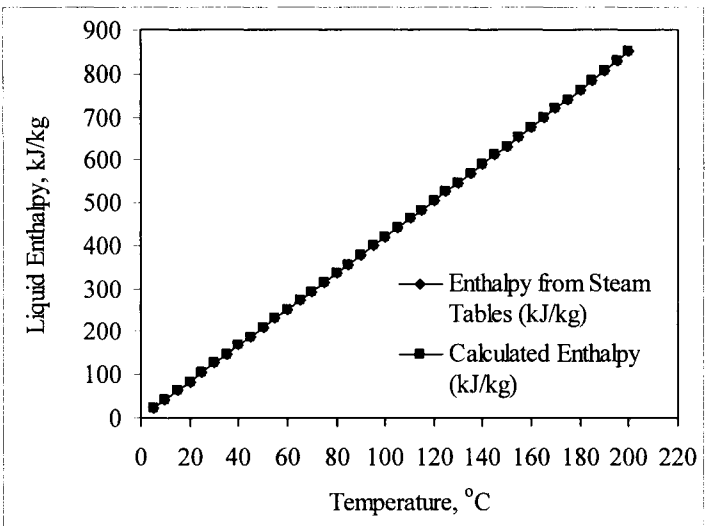

Figure A.5: Variation in enthalpy of liquid water as a function of temperature.

Table A.5: Variation in liquid water enthalpy (kJ/kg) as a function of temperature (°C).

T (°C)	Calculated Enthalpy (kJ/kg)	Enthalpy from Steam Tables (kJ/kg)	Percentage Error
5	20.98921	20.98	0.043881
10	41.98439	41.99	0.013359
15	62.95526	62.98	0.039278
20	83.90517	83.94	0.041498
25	104.8374	104.87	0.031042
30	125.7554	125.77	0.011571
35	146.6625	146.66	0.001714
40	167.562	167.54	0.013126
45	188.4572	188.42	0.019755
50	209.3516	209.31	0.019852
55	230.2483	230.2	0.020993
60	251.1509	251.11	0.016283
65	272.0626	272.03	0.011978
70	292.9868	292.96	0.009133
75	313.9267	313.91	0.005335
80	334.8859	334.88	0.001764
85	355.8676	355.88	0.00349
90	376.8751	376.9	0.006605
95	397.9118	397.94	0.007079
100	418.9811	419.02	0.009283
105	440.0863	440.13	0.009938
110	461.2307	461.27	0.00853
115	482.4176	482.46	0.008783
120	503.6505	503.69	0.007839
125	524.9327	524.96	0.005205
130	546.2674	546.29	0.004128
135	567.6582	567.67	0.002083
140	589.1082	589.11	0.000305
145	610.6209	610.61	0.001782
150	632.1995	632.18	0.003091
155	653.8475	653.82	0.004212
160	675.5682	675.53	0.005657
165	697.3649	697.32	0.006441
170	719.241	719.2	0.005699
175	741.1998	741.16	0.005365
180	763.2446	763.21	0.004534
185	785.3788	785.36	0.002399
190	807.6058	807.61	0.000517
195	829.9289	829.96	0.003747
200	852.3514	852.43	0.00922

A.6. Enthalpy of Saturated Water Vapor

The correlation for the water vapor enthalpy is given by

$$H'' = 2501.689845 + 1.806916015\ T + 5.087717\text{x}10^{-4}\ T^2 - 1.1221\text{x}10^{-5}\ T^3 \quad \text{(A.6)}$$

In the above equation, T is the saturation temperature in °C and H" is the vapor enthalpy in kJ/kg. Values for the calculated enthalpy over a temperature range of 0.01–200 °C are given in Table A.6. The table also includes values extracted from the steam tables. The percentage errors for the calculated versus the steam table values are less than 0.017%. Figure A.6 show variations in the calculated and the steam table values for the enthalpy of water vapor as a function of temperature.

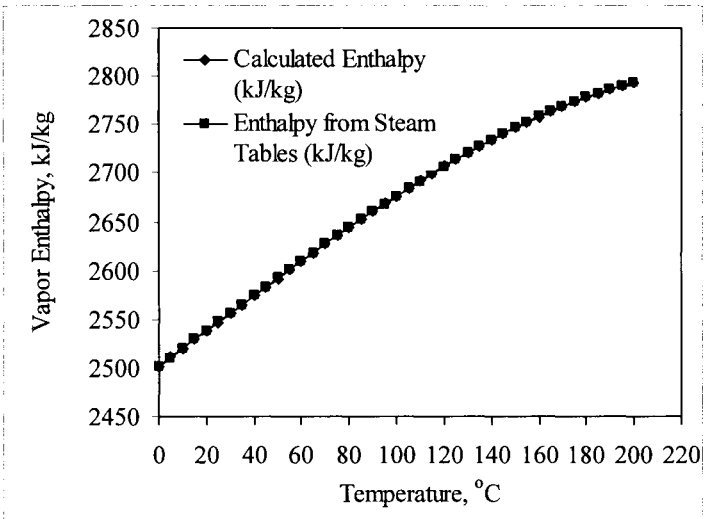

Figure A.6: Variation in enthalpy of water vapor as a function of temperature.

Table A.6: Variation in water vapor enthalpy (kJ/kg) as a function of temperature (°C)

T (°C)	Calculated Enthalpy (kJ/kg)	Enthalpy from Steam Tables (kJ/kg)	Percentage Error
0.01	2501.708	2501.35	0.014309
5	2510.736	2510.54	0.007797
10	2519.799	2519.74	0.002328
15	2528.87	2528.91	0.001574
20	2537.942	2538.06	0.004653
25	2547.005	2547.17	0.006462
30	2556.052	2556.25	0.007736
35	2565.074	2565.28	0.008028
40	2574.062	2574.26	0.007677
45	2583.009	2583.19	0.007014
50	2591.905	2592.06	0.005982
55	2600.742	2600.86	0.004523
60	2609.513	2609.59	0.002964
65	2618.207	2618.24	0.001246
70	2626.818	2626.8	0.000691
75	2635.337	2635.28	0.002146
80	2643.754	2643.66	0.003561
85	2652.063	2651.93	0.004997
90	2660.253	2660.09	0.006137
95	2668.318	2668.13	0.007044
100	2676.248	2676.05	0.007406
105	2684.036	2683.83	0.007659
110	2691.672	2691.47	0.007492
115	2699.148	2698.96	0.006966
120	2706.456	2706.3	0.005773
125	2713.588	2713.46	0.004715
130	2720.535	2720.46	0.002746
135	2727.288	2727.26	0.00103
140	2733.84	2733.87	0.001109
145	2740.181	2740.26	0.002881
150	2746.304	2746.44	0.004958
155	2752.2	2752.39	0.006918
160	2757.86	2758.09	0.008344
165	2763.276	2763.53	0.00918
170	2768.44	2768.7	0.009375
175	2773.344	2773.58	0.008513
180	2777.978	2778.16	0.006543
185	2782.335	2782.43	0.003413
190	2786.406	2786.37	0.001289
195	2790.182	2789.96	0.007972
200	2793.656	2793.18	0.017047

A.7. Latent Heat of Water Evaporation

The correlation for latent heat of water evaporation is given by

$$\lambda = 2501.897149 - 2.407064037\,T + 1.192217\times10^{-3}\,T^2 - 1.5863\times10^{-5}\,T^3 \quad (A.7)$$

In the above equation, T is the saturation temperature in °C and λ is the latent heat in kJ/kg. Values for the calculated enthalpy over a temperature range of 5–200 °C are given in Table A.7. The table also includes values extracted from the steam tables. The percentage errors for the calculated versus the steam table values are less than 0.026%. Figure A.7 show variations in the calculated and the steam table values for the latent heat of water as a function of temperature.

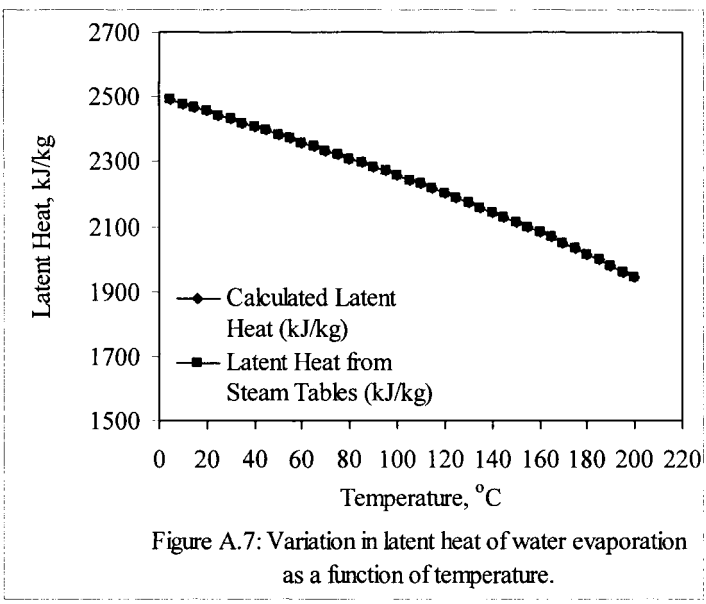

Figure A.7: Variation in latent heat of water evaporation as a function of temperature.

Table A.7: Variation in latent heat of water evaporation in (kJ/kg) as a function of temperature (°C)

T (°C)	Calculated Latent Heat (kJ/kg)	Latent Heat from Steam Tables (kJ/kg)	Percentage Error
5	2489.89	2489.56	0.013241
10	2477.93	2477.75	0.007259
15	2466.006	2465.93	0.003078
20	2454.106	2454.12	0.000577
25	2442.218	2442.3	0.003365
30	2430.33	2430.48	0.006175
35	2418.43	2418.62	0.007845
40	2406.507	2406.72	0.008854
45	2394.548	2394.77	0.009271
50	2382.542	2382.75	0.008746
55	2370.476	2370.66	0.007767
60	2358.339	2358.48	0.005984
65	2346.119	2346.21	0.00389
70	2333.804	2333.84	0.001563
75	2321.381	2321.37	0.000489
80	2308.84	2308.78	0.002614
85	2296.169	2296.05	0.005166
90	2283.354	2283.19	0.007192
95	2270.385	2270.19	0.008602
100	2257.25	2257.03	0.009743
105	2243.936	2243.7	0.010528
110	2230.432	2230.2	0.010415
115	2216.726	2216.5	0.010206
120	2202.806	2202.61	0.008904
125	2188.66	2188.5	0.007316
130	2174.276	2174.17	0.004888
135	2159.643	2159.59	0.002441
140	2144.748	2144.76	0.00058
145	2129.579	2129.65	0.00334
150	2114.125	2114.26	0.006395
155	2098.373	2098.57	0.009369
160	2082.313	2082.56	0.01187
165	2065.931	2066.21	0.013499
170	2049.216	2049.5	0.013838
175	2032.157	2032.42	0.01295
180	2014.74	2014.95	0.010402
185	1996.955	1997.07	0.005742
190	1978.79	1978.76	0.001499
195	1960.232	1960	0.011812
200	1941.269	1940.75	0.026741

A.8. Entropy of Saturated Liquid Water

The correlation for entropy of saturated liquid water is given by

$$S = -0.00057846 + 0.015297489\,T - 2.63129\times10^{-5}\,T^2 + 4.11959\times10^{-8}\,T^3 \quad \text{(A.8)}$$

In the above equation, T is the saturation temperature in °C and S is the entropy of saturated liquid water in kJ/kg °C. Values for the calculated entropy over a temperature range of 5–200 °C are given in Table A.8. The table also includes values extracted from the steam tables. The percentage errors for the calculated versus the steam table values are less than 0.4%. Figure A.8 show variations in the calculated and the steam table values for the saturation entropy of water vapor as a function of temperature.

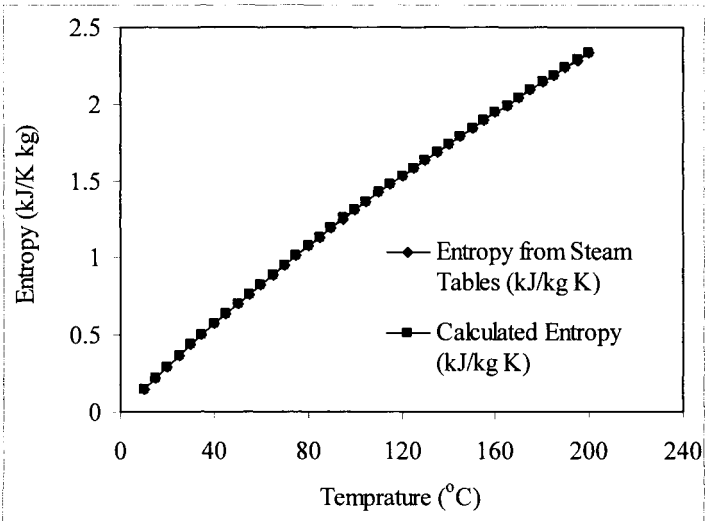

Figure A.8: Variation in entropy of saturated liquid water as a function of temperature

Table A.8: Variation in the entropy of saturated liquid water (kJ/kg °C) as a function of temperature (°C)

T (°C)	Entropy from Steam Table (kJ/kg °C)	Calculated Entropy (kJ/kg °C)	Percentage Error
10	0.149806	0.151	0.790506
15	0.223103	0.2245	0.62249
20	0.295176	0.2966	0.4802
25	0.366057	0.3673	0.338446
30	0.435777	0.4369	0.257064
35	0.504367	0.5052	0.16496
40	0.571857	0.5724	0.094865
45	0.638279	0.6386	0.050283
50	0.703663	0.7037	0.005227
55	0.768041	0.7679	0.018345
60	0.831443	0.8311	0.041239
65	0.8939	0.8934	0.055935
70	0.955443	0.9548	0.067316
75	1.016103	1.0154	0.069199
80	1.07591	1.0752	0.066068
85	1.134897	1.1342	0.061435
90	1.193093	1.1924	0.058103
95	1.250529	1.25	0.042348
100	1.307237	1.3068	0.033462
105	1.363247	1.3629	0.025497
110	1.418591	1.4184	0.013459
115	1.473298	1.4733	0.000109
120	1.527401	1.5275	0.006489
125	1.580929	1.5812	0.017124
130	1.633914	1.6343	0.023596
135	1.686387	1.6869	0.0304
140	1.738379	1.739	0.035735
145	1.789919	1.7906	0.038009
150	1.841041	1.8417	0.035802
155	1.891773	1.8924	0.033127
160	1.942148	1.9426	0.023281
165	1.992195	1.9924	0.010267
170	2.041947	2.0418	0.007203
175	2.091434	2.0909	0.025519
180	2.140686	2.1395	0.055425
185	2.189735	2.1878	0.088431
190	2.238611	2.2358	0.125732
195	2.287346	2.2835	0.168425
200	2.33597	2.3308	0.22182

A.9. Entropy of Saturated Water Vapor

The correlation for entropy of saturated water vapor is given by

$$S = 9.149505306 - 2.581012 \times 10^{-2} T + 9.625687 \times 10^{-5} T^2 - 1.786615 \times 10^{-7} T^3 \quad \text{(A.9)}$$

In the above equation, T is the saturation temperature in °C and S is the entropy of saturated water vapor in kJ/kg K. Values for the calculated entropy over a temperature range of 0.01–200 °C are given in Table A.9. The table also includes values extracted from the steam tables. The percentage errors for the calculated versus the steam table values are less than 0.4%. Figure A.9 show variations in the calculated and the steam table values for the saturation entropy of water vapor as a function of temperature.

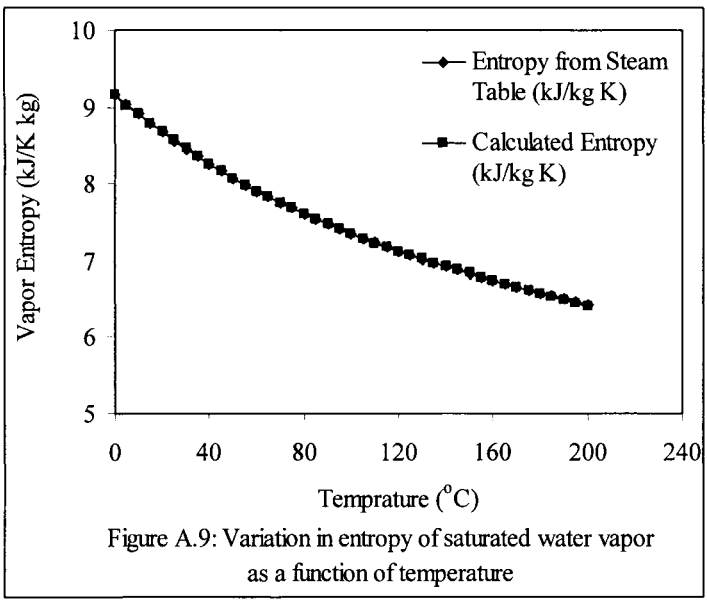

Figure A.9: Variation in entropy of saturated water vapor as a function of temperature

Table A.9: Variation in the entropy of saturated water vapor (kJ/kg K) as a function of temperature (°C)

T (°C)	Entropy from Steam Table (kJ/kg °C)	Calculated Entropy (kJ/kg K)	Percentage Error
0.01	9.1562	9.14925	0.07594
5	9.0257	9.02284	0.03170
10	8.9007	8.90085	0.00170
15	8.7813	8.78341	0.02401
20	8.6671	8.67038	0.03780
25	8.5579	8.56162	0.04348
30	8.4533	8.45701	0.04388
35	8.353	8.35641	0.04077
40	8.2569	8.25968	0.03363
45	8.1647	8.16669	0.02437
50	8.0762	8.07731	0.01373
55	7.9912	7.99140	0.00251
60	7.9095	7.90883	0.00845
65	7.8309	7.82947	0.01829
70	7.7552	7.75317	0.02612
75	7.6824	7.67982	0.03361
80	7.6121	7.60926	0.03725
85	7.5444	7.54138	0.04003
90	7.479	7.47603	0.03970
95	7.4158	7.41308	0.03665
100	7.3548	7.35240	0.03263
105	7.2958	7.29385	0.02671
110	7.2386	7.23730	0.01794
115	7.1832	7.18262	0.00812
120	7.1295	7.12966	0.00228
125	7.0774	7.07831	0.01279
130	7.0269	7.02841	0.02150
135	6.977	6.97985	0.04079
140	6.9298	6.93248	0.03861
145	6.8832	6.88617	0.04309
150	6.8378	6.84078	0.04364
155	6.7934	6.79619	0.04113
160	6.7501	6.75226	0.03206
165	6.7078	6.70886	0.01578
170	6.6663	6.66584	0.00684
175	6.6256	6.62309	0.03794
180	6.5857	6.58045	0.07969
185	6.5464	6.53781	0.13128
190	6.5078	6.49502	0.19645
195	6.4697	6.45195	0.27442
200	6.4322	6.40846	0.36903

A.10. Saturation Pressure of Water Vapor

The correlation for the water vapor saturation pressure is given by

$$\ln(P/P_c) = \left(\frac{T_c}{T+273.15} - 1\right) \sum_{i=1}^{8} f_i (0.01(T+273.15-338.15))^{(i-1)} \quad \text{(A.10)}$$

where T_c = 647.286 K and P_c = 22089 kPa and the values of f_i are given in the following tables

f_1	f_2	f_3	f_4
-7.419242	0.29721	-0.1155286	0.008685635
f_5	f_6	f_7	f_8
0.001094098	-0.00439993	0.002520658	-0.000521868

where P is kPa and T is °C. Values for the calculated vapor pressure over a temperature range of 5-200 °C are given in table A.10. The table also includes values extracted from the steam tables. The percentage errors for the calculated versus the steam table values are less than 0.05%. Figure A.10 shows variations in the calculated and the steam table values for the vapor pressure of water as a function of temperature.

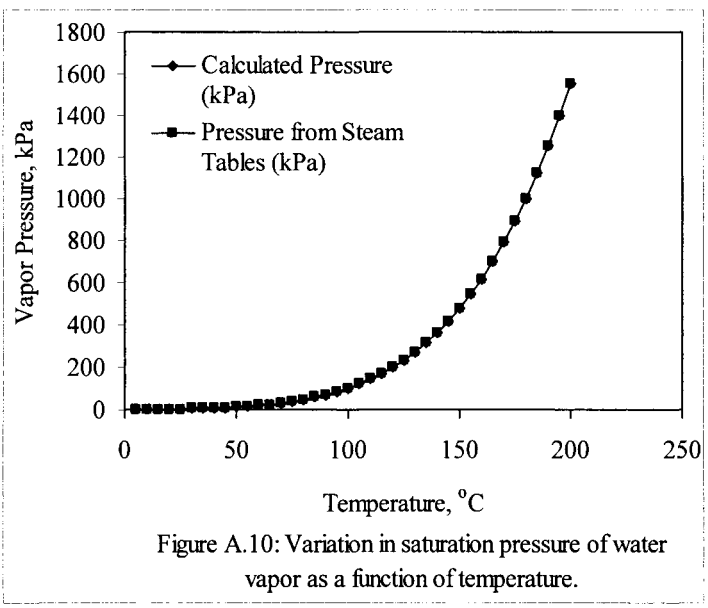

Figure A.10: Variation in saturation pressure of water vapor as a function of temperature.

Table A.10: Variation in saturation pressure of water vapor (kPa) as a function of temperature (°C)

T (°C)	Calculated Pressure (kPa)	Pressure from Steam Tables (kPa)	Percentage Error
5	0.872	0.8721	1.04E-04
10	1.228	1.2276	1.23E-03
15	1.705	1.705	3.76E-03
20	2.339	2.339	2.12E-02
25	3.169	3.169	1.61E-03
30	4.246	4.246	5.81E-04
35	5.628	5.628	8.74E-04
40	7.384	7.384	5.03E-03
45	9.593	9.593	2.26E-03
50	12.349	12.35	5.41E-03
55	15.758	15.758	8.65E-04
60	19.940	19.941	2.93E-03
65	25.033	25.03	1.05E-02
70	31.188	31.19	6.73E-03
75	38.577	38.58	7.77E-03
80	47.389	47.39	1.63E-03
85	57.833	57.83	5.57E-03
90	70.138	70.14	3.22E-03
95	84.552	84.55	2.72E-03
100	101.348	101.3	4.72E-02
105	120.817	120.8	1.40E-02
110	143.275	143.3	1.77E-02
115	169.059	169.1	2.45E-02
120	198.529	198.5	1.46E-02
125	232.069	232.1	1.32E-02
130	270.086	270.1	5.30E-03
135	313.007	313	2.39E-03
140	361.287	361.3	3.59E-03
145	415.399	415.4	1.34E-04
150	475.843	475.9	1.21E-02
155	543.137	543.1	6.79E-03
160	617.825	617.8	4.03E-03
165	700.471	700.5	4.08E-03
170	791.663	791.7	4.68E-03
175	892.008	892	8.53E-04
180	1002.135	1002.2	6.50E-03
185	1122.695	1122.7	4.07E-04
190	1254.361	1254.4	3.13E-03
195	1397.823	1397.8	1.65E-03
200	1553.795	1553.8	2.95E-04

A.11. Saturation Temperature of Water Vapor

The correlation for the saturation temperature of water vapor is given by

$$T = \left(42.6776 - \frac{3892.7}{(\ln(P/1000) - 9.48654)} \right) - 273.15 \qquad (A.11)$$

where P is in kPa and T is in °C. Values for the calculated saturation temperature over a pressure range of 0.8721-1553.8 kPa and a temperature range of 5-200 °C are given in Table A.11. The table also includes values extracted from the steam tables. The percentage errors for the calculated versus the steam table values are less than 0.28%. Figure A.11 shows variations in the calculated and the steam table values for the vapor pressure of water as a function of temperature.

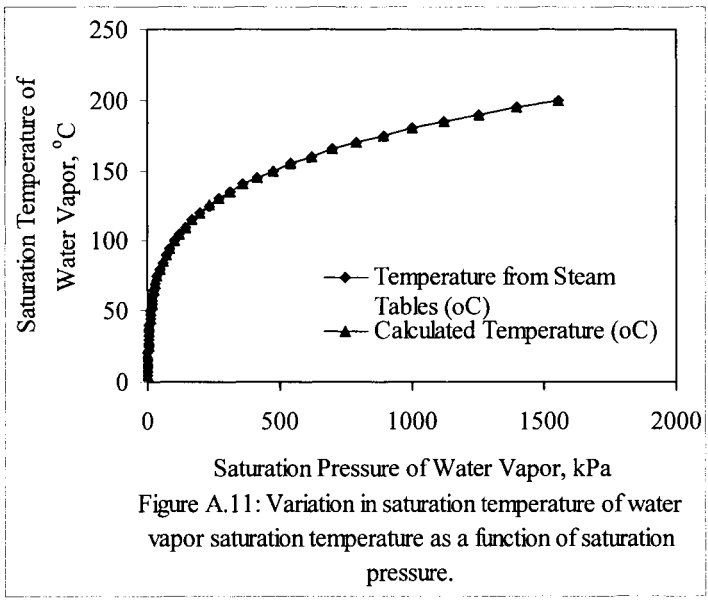

Figure A.11: Variation in saturation temperature of water vapor saturation temperature as a function of saturation pressure.

Table A.11: Variation in saturation temperature of water vapor (°C) as a function of saturation pressure (kPa)

P (kPa)	Calculated Temperature (°C)	Temperature from Steam Tables (°C)	Percentage Error
0.8721	5.004311	5	0.086223
1.2276	9.977515	10	0.224847
1.705	14.95766	15	0.282249
2.339	19.94942	20	0.252887
3.169	24.93937	25	0.242502
4.246	29.93817	30	0.206098
5.628	34.94124	35	0.167899
7.384	39.94826	40	0.129338
9.593	44.95588	45	0.098035
12.35	49.96858	50	0.062849
15.758	54.98005	55	0.036268
19.941	59.99471	60	0.008819
25.03	65.00619	65	0.009523
31.19	70.02479	70	0.035412
38.58	75.03961	75	0.052814
47.39	80.05217	80	0.065212
57.83	85.06355	85	0.074765
70.14	90.07795	90	0.086612
84.55	95.08715	95	0.091739
101.3	100.0839	100	0.083897
120.8	105.1006	105	0.095797
143.3	110.1155	110	0.105
169.1	115.1213	115	0.105474
198.5	120.1106	120	0.092129
232.1	125.1186	125	0.094893
270.1	130.1129	130	0.086868
313	135.1048	135	0.077651
361.3	140.0991	140	0.070757
415.4	145.0877	145	0.060451
475.9	150.0796	150	0.053085
543.1	155.0579	155	0.037346
617.8	160.0422	160	0.026344
700.5	165.0267	165	0.016166
791.7	170.0065	170	0.00382
892	174.9822	175	0.010192
1002.2	179.962	180	0.021134
1122.7	184.9349	185	0.0352
1254.4	189.9109	190	0.046896
1397.8	194.883	195	0.059982
1553.8	199.8582	200	0.070913

A.12. Specific Volume of Saturated Water Vapor

The correlation for the specific volume of saturated water vapor is given by

$$V = V_c\left(\frac{T_c}{T+273.15} - 1\right) \exp\left(\sum_{i=1}^{6} f_i (T+273.15)^{(i-1)}\right) \qquad (A.12)$$

where T_c = 647.286 K and V_c = 0.003172222 m^3/kg and the values of f_i are given in the following tables

f_1	f_2	f_3	f_4	f_5	f_6
83.63213098	-0.668265339	0.002495964	-5.04185E-06	5.34205E-09	-2.3279E-12

where V is in m^3/kg and T is in °C. Values for the calculated saturation vapor volumes over a temperature range of 5-200 °C are given in Table A.12. The table also includes values extracted from the steam tables. The percentage errors for the calculated versus the steam table values are less than 0.025%. Figure A.12 shows variations in the calculated and the steam table values for the saturation volume of water vapor as a function of temperature.

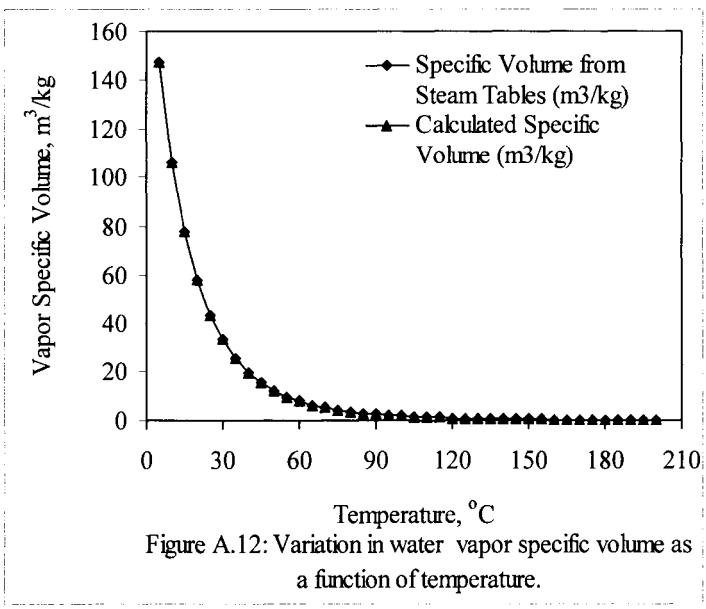

Figure A.12: Variation in water vapor specific volume as a function of temperature.

Table A.12: Variation in water vapor specific volume (m^3/kg) as a function of temperature (°C)

T (°C)	Calculated Specific Volume (m^3/kg)	Specific Volume from Steam Tables (m^3/kg)	Percentage Error
5	147.07980	147.117	0.025285
10	106.37933	106.376	0.003132
15	77.93664	77.925	0.014937
20	57.79982	57.7897	0.017517
25	43.36557	43.3593	0.014456
30	32.89601	32.8932	0.008551
35	25.21619	25.2158	0.001542
40	19.52198	19.5229	0.004735
45	15.25660	15.2581	0.009804
50	12.03025	12.0318	0.012911
55	9.56703	9.56835	0.013787
60	7.66972	7.67071	0.012893
65	6.19591	6.19656	0.010432
70	5.04182	5.04217	0.00686
75	4.13113	4.13123	0.002424
80	3.40722	3.40715	0.001964
85	2.82774	2.82757	0.006085
90	2.36078	2.36056	0.009443
95	1.98209	1.98186	0.011582
100	1.67311	1.6729	0.012267
105	1.41953	1.41936	0.011962
110	1.21027	1.21014	0.010649
115	1.03666	1.03658	0.007642
120	0.89189	0.89186	0.003796
125	0.77059	0.77059	0.000286
130	0.66848	0.6685	0.003484
135	0.58213	0.58217	0.007239
140	0.50880	0.50885	0.010324
145	0.44627	0.44632	0.012189
150	0.39273	0.39278	0.012698
155	0.34672	0.34676	0.0112
160	0.30703	0.30706	0.008363
165	0.27268	0.27269	0.004259
170	0.24283	0.24283	0.001703
175	0.21682	0.2168	0.010016
180	0.19407	0.19405	0.012725
185	0.17412	0.17409	0.016859
190	0.15656	0.15654	0.011531
195	0.14106	0.14105	0.004138
200	0.12733	0.12736	0.023873

A.13. Specific Volume of Saturated Liquid Water

The correlation for the specific volume of saturated liquid water is given by

$$V = V_c\left(\frac{T_c}{T+273.15} - 1\right) \exp\left(\sum_{i=1}^{6} f_i (T+273.15)^{(i-1)}\right) \quad \text{(A.13)}$$

where T_c = 647.286 K and V_c = 0.003172222 m^3/kg and the values of f_i are given in the following tables

f_1	f_2	f_3	f_4	f_5	f_6
-2.781015567	0.002543267	9.845047E-06	3.636115E-09	-5.358938E-11	7.019341E-14

In the above equation V is in m^3/kg and T is in °C. Values for the calculated saturation volumes over a temperature range of 5-200 °C are given in Table A.13. The table also includes values extracted from the steam tables. The percentage errors for the calculated versus the steam table values are less than 0.05%. Figure A.13 shows variations in the calculated and the steam table values for the saturation volume of liquid water as a function of temperature.

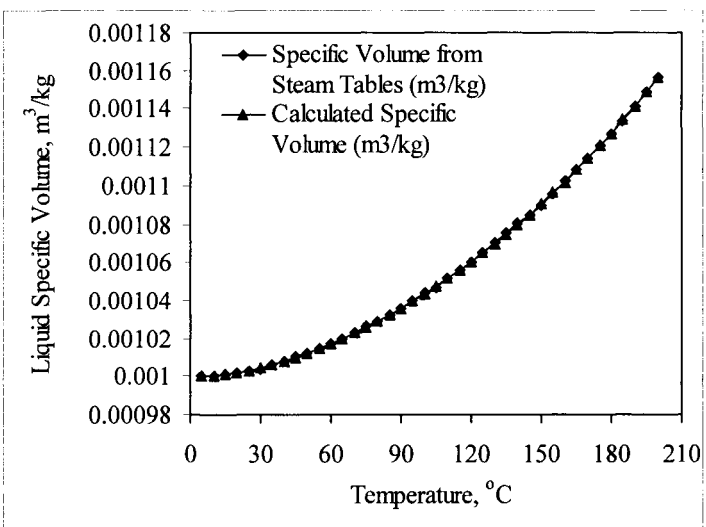

Figure A.13: Variation in liquid water specific volume as a function of temperature.

Table A.13: Variation in liquid water specific volume (m^3/kg) as a function of temperature (^oC)

T (^oC)	Calculated Specific Volume (m^3/kg)	Specific Volume from Steam Tables (m^3/kg)	Percentage Error
5	0.001000	0.001	0.013868
10	0.001000	0.001	0.024433
15	0.001001	0.001001	0.009436
20	0.001002	0.001002	0.017042
25	0.001003	0.001003	8.72E-05
30	0.001004	0.001004	0.040541
35	0.001006	0.001006	0.003518
40	0.001008	0.001008	0.012434
45	0.001010	0.00101	0.008456
50	0.001012	0.001012	0.014415
55	0.001015	0.001015	0.043332
60	0.001017	0.001017	0.014757
65	0.001020	0.00102	0.008914
70	0.001023	0.001023	0.016466
75	0.001026	0.001026	0.008502
80	0.001029	0.001029	0.014466
85	0.001033	0.001032	0.052013
90	0.001036	0.001036	0.007174
95	0.001040	0.00104	0.023063
100	0.001044	0.001044	0.038921
105	0.001048	0.001047	0.054927
110	0.001052	0.001052	0.028004
115	0.001056	0.001056	0.001294
120	0.001060	0.00106	0.039654
125	0.001065	0.001065	0.00099
130	0.001070	0.00107	0.022361
135	0.001075	0.001075	0.030203
140	0.001080	0.00108	0.022294
145	0.001085	0.001085	0.001649
150	0.001090	0.00109	0.041944
155	0.001096	0.001096	0.007601
160	0.001102	0.001102	0.008834
165	0.001108	0.001108	0.007062
170	0.001114	0.001114	0.013203
175	0.001121	0.001121	0.037027
180	0.001127	0.001127	0.021395
185	0.001134	0.001134	0.01066
190	0.001141	0.001141	0.020023
195	0.001149	0.001149	0.037698
200	0.001156	0.001156	0.011881

A.14. Dynamic Viscosity of Saturated Liquid Water

The correlation for the dynamic viscosity of saturated liquid water is given by

$$\mu = \exp(-3.79418 + 604.129/(139.18+T)) \times 10^{-3} \quad \text{(A.14)}$$

where μ in kg/m s, and T in °C. The above correlation is valid over a temperature range of 10-115 °C. Variations in the dynamic viscosity of saturated water as a function of temperature are given in Table A.14 and Fig. A.14.

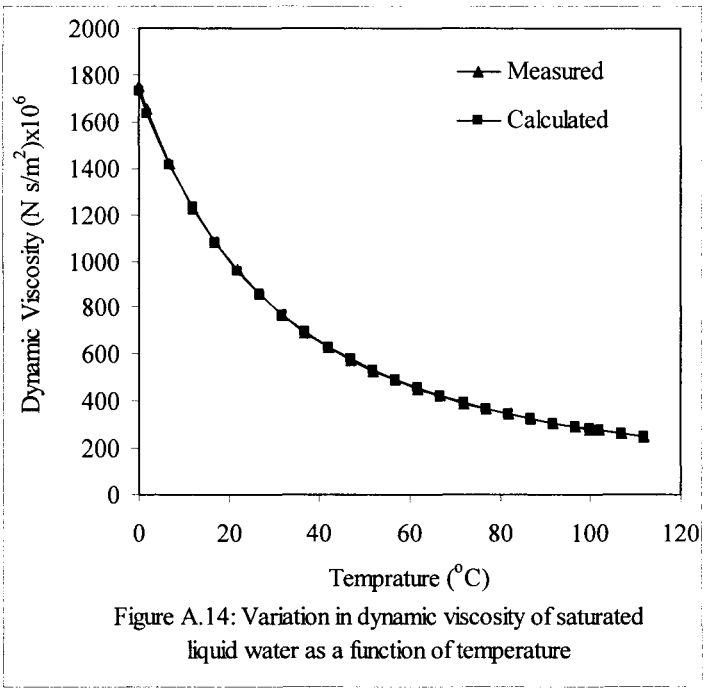

Figure A.14: Variation in dynamic viscosity of saturated liquid water as a function of temperature

Table A.14: Variation in liquid water dynamic viscosity as a function of temperature

T (°C)	Calculated Dynamic Viscosity ($N.s/m^2$)$x10^6$	Measured Dynamic Viscosity ($N.s/m^2$)$x10^6$	Percentage Error
11.85	1228.605	1225	0.294307
16.85	1080.795	1080	0.073643
21.85	958.3665	959	0.066061
26.85	855.9817	855	0.11482
31.85	769.6022	769	0.078304
36.85	696.1335	695	0.16309
41.85	633.1779	631	0.345152
46.85	578.8578	577	0.321977
51.85	531.6884	528	0.698561
56.85	490.4848	489	0.30365
61.85	454.2936	453	0.285561
66.85	422.3411	420	0.557407
71.85	393.9953	389	1.284127
76.85	368.7358	365	1.023506
81.85	346.1318	343	0.913062
86.85	325.8241	324	0.562993
91.85	307.5116	306	0.493979
96.85	290.9404	289	0.671431
100	281.2965	279	0.823129
101.85	275.8956	274	0.691832
106.85	262.194	260	0.843854
111.85	249.679	248	0.677015

A.15. Dynamic Viscosity of Saturated Water Vapor

The correlation for the dynamic viscosity of saturated water vapor is given by

$$\mu = \exp(-3.609417664 + 275.928958/(-227.0446083 - 0.896081232T - 0.002291383T^2)) \times 10^{-3} \quad \text{(A.15)}$$

where μ in kg/m s, and T in °C. The above correlation is valid over the following a temperature range of 10-180 °C. Variations in the saturated water dynamic viscosity as a function of temperature are given in Table A.15 and Fig. A.15.

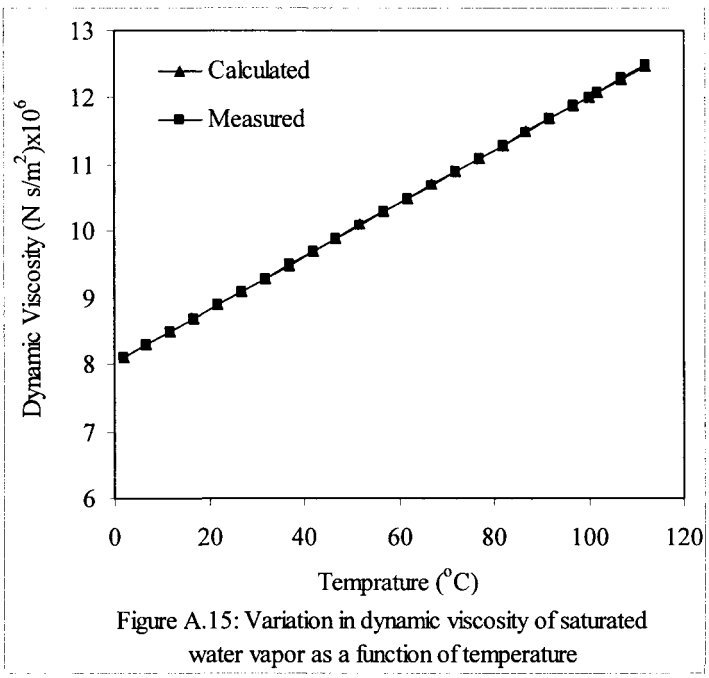

Figure A.15: Variation in dynamic viscosity of saturated water vapor as a function of temperature

Table A.15: Variation in the dynamic viscosity of saturated water vapor as a function of temperature.

T (°C)	Calculated Dynamic Viscosity ($N.s/m^2$)$x10^6$	Measured Dynamic Viscosity ($N.s/m^2$)$x10^6$	Percentage Error
1.85	8.100136375	8.09	0.125295
6.85	8.294284892	8.29	0.051687
11.85	8.490083562	8.49	0.000984
16.85	8.687322522	8.69	0.030811
21.85	8.885795492	8.89	0.047295
26.85	9.085300391	9.09	0.051701
31.85	9.285639887	9.29	0.046933
36.85	9.486621888	9.49	0.035597
41.85	9.688059977	9.69	0.020021
46.85	9.88977379	9.89	0.002287
51.85	10.09158933	10.09	0.015752
56.85	10.29333925	10.29	0.032451
61.85	10.49486302	10.49	0.046359
66.85	10.69600714	10.69	0.056194
71.85	10.89662523	10.89	0.060838
76.85	11.09657809	11.09	0.059315
81.85	11.29573373	11.29	0.050786
86.85	11.4939674	11.49	0.034529
91.85	11.69116147	11.69	0.009936
96.85	11.88720544	11.89	0.023503
100	12.01007572	12.02	0.082565
101.85	12.08199576	12.09	0.066205
106.85	12.27543577	12.29	0.118505
111.85	12.46743551	12.49	0.18066

A.16. Surface Tension of Saturated Liquid Water

The correlation for the surface tension is given by

$$\sigma = 7.5798 \times 10^{-2} - 1.4691 \times 10^{-4}\, T - 2.2173 \times 10^{-7}\, T^2 \qquad \text{(A.16)}$$

where σ in N/m, and T in °C. The above correlation is valid over the following a temperature range of 0-136 °C. Variations in the saturated water surface tension as a function of temperature are given in Table A.16 and Fig. A.16.

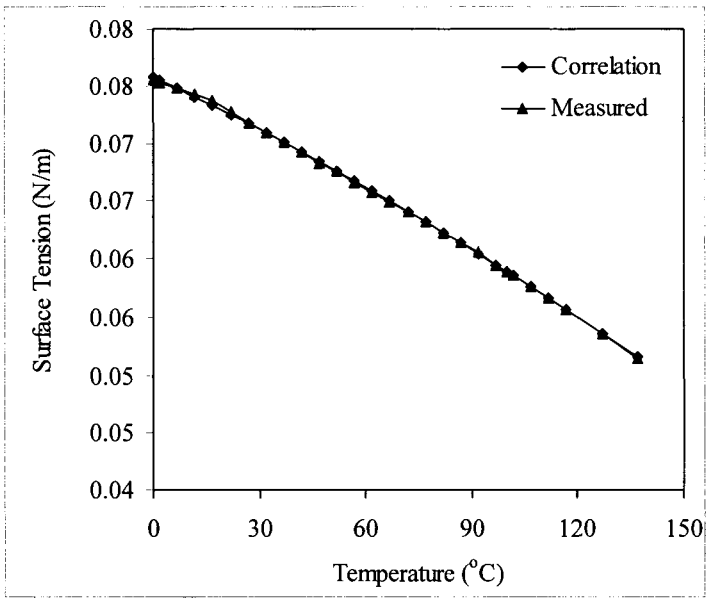

Figure A.16: Variation in surface tension of saturated liquid water as a function of temperature.

Table A.16: Variation in the surface tension of saturated liquid water as a function of temperature.

T (°C)	Measured	Correlation	error%
0	7.55E-02	7.58E-02	3.95E-01
1.85	7.53E-02	7.55E-02	3.00E-01
6.85	7.48E-02	7.48E-02	2.47E-02
11.85	7.43E-02	7.40E-02	3.68E-01
16.85	7.37E-02	7.33E-02	5.97E-01
21.85	7.27E-02	7.25E-02	2.99E-01
26.85	7.17E-02	7.17E-02	8.63E-03
31.85	7.09E-02	7.09E-02	8.22E-03
36.85	7.00E-02	7.01E-02	1.19E-01
41.85	6.92E-02	6.93E-02	8.91E-02
46.85	6.83E-02	6.84E-02	1.88E-01
51.85	6.75E-02	6.76E-02	1.26E-01
56.85	6.66E-02	6.67E-02	1.95E-01
61.85	6.58E-02	6.59E-02	9.65E-02
66.85	6.49E-02	6.50E-02	1.33E-01
71.85	6.41E-02	6.41E-02	3.23E-03
76.85	6.32E-02	6.32E-02	2.36E-03
81.85	6.23E-02	6.23E-02	1.93E-02
86.85	6.14E-02	6.14E-02	5.47E-02
91.85	6.05E-02	6.04E-02	1.10E-01
96.85	5.95E-02	5.95E-02	1.69E-02
100	5.89E-02	5.89E-02	1.75E-02
101.85	5.86E-02	5.85E-02	1.11E-01
106.85	5.76E-02	5.76E-02	5.35E-02
111.85	5.66E-02	5.66E-02	1.39E-02
116.85	5.56E-02	5.56E-02	7.28E-03
126.85	5.36E-02	5.36E-02	1.01E-02
136.85	5.15E-02	5.15E-02	7.91E-02

A.17. Enthalpy of LiBr Water Solution

The enthalpy correlation for saturated LiBr-H_2O solution is given by

$$H(X,T) = X\sum_{i=0}^{4} a_i T^i + (1-X)\sum_{i=0}^{2} b_i T^i + X(1-X)\sum_{i=0}^{4}\sum_{j=0}^{3} c_{ij}(2X-1)^i\, T^j \qquad \text{(A.17)}$$

where X is the mass fraction of LiBr and T is the solution temperature. The constants in the above relation are as follows:

$a_0 = 508.668$, $a_1 = 18.6241$, $a_2 = 0.0985946$, $a_3 = -2.500979\text{x}10^{-5}$,
$a_4 = 4.15801\text{x}10^{-8}$, $b_1 = 1.617155702$, $b_2 = 4.10187485$, $b_3 = 0.000717667$,
$c_{00} = -1021.61$, $c_{10} = -533.08$, $c_{20} = 483.628$, $c_{30} = 1155.13$, $c_{40} = 640.622$,
$c_{01} = 36.8773$, $c_{11} = 40.2847$, $c_{21} = 39.9142$, $c_{31} = 33.3572$, $c_{41} = 13.1032$,
$c_{02} = -0.186051$, $c_{12} = -0.191198$, $c_{22} = 0.199213$, $c_{32} = -0.178258$,
$c_{42} = -0.0775101$, $c_{03} = -7.51277\text{E}{-6}$, $c_{13} = 0$, $c_{23} = 0$, $c_{33} = 0$, $c_{43} = 0$

The enthalpy of the saturated LiBr solution are shown in Table A.17 and Fig. A.17 for a temperature range of 10-170 °C and LiBr mass fraction of 0.25-0.75.

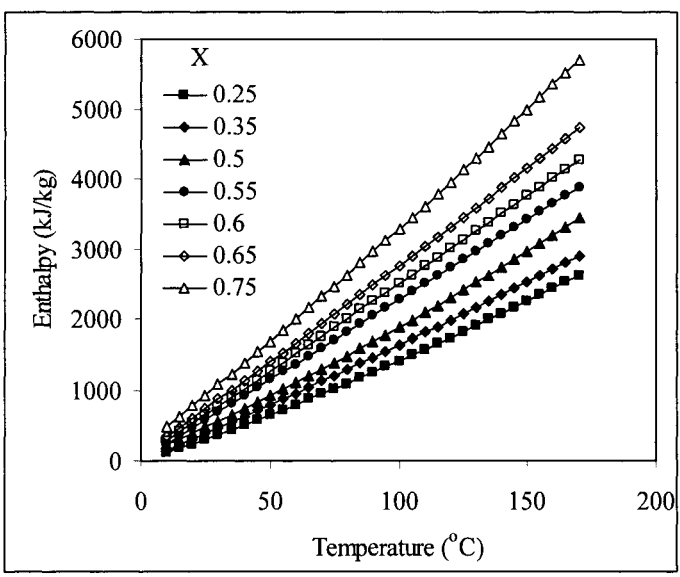

Fig. A.17. Variation in the enthalpy of LiBr solution as a function of temperature and mass fraction

Table A.17: Variation in enthalpy of saturated LiBr solution as a function of temperature (°C) and LiBr mass fraction

	LiBr mass fraction										
T (°C)	0.25	0.3	0.35	0.4	0.45	0.5	0.55	0.6	0.65	0.7	0.75
10	113.11	127.53	142.71	159.68	180.03	205.86	239.56	283.4	339.01	406.79	485.08
15	176.27	198.39	221.34	246.24	274.78	309.13	351.66	404.51	469.08	545.27	630.68
20	240.44	270.01	300.47	333.1	369.71	412.53	463.93	525.95	599.69	684.61	777.52
25	305.64	342.4	380.12	420.26	464.8	516.05	576.37	647.69	730.85	824.79	925.58
30	371.85	415.54	460.26	507.72	560.04	619.67	688.96	769.74	862.54	965.81	1074.9
35	439.07	489.43	540.9	595.45	655.43	723.39	801.71	892.07	994.74	1107.6	1225.3
40	507.3	564.07	622.02	683.46	750.95	827.19	914.58	1014.7	1127.4	1250.3	1377
45	576.53	639.44	703.63	771.74	846.61	931.08	1027.6	1137.6	1260.7	1393.7	1529.8
50	646.75	715.55	785.71	860.28	942.39	1035	1140.7	1260.7	1394.3	1538	1683.8
55	717.97	792.38	868.26	949.07	1038.3	1139.1	1254	1384.1	1528.5	1683	1838.9
60	790.17	869.94	951.27	1038.1	1134.3	1243.2	1367.3	1507.7	1663.1	1828.8	1995.2
65	863.36	948.22	1034.7	1127.4	1230.4	1347.3	1480.7	1631.6	1798.2	1975.3	2152.6
70	937.53	1027.2	1118.7	1216.9	1326.6	1451.5	1594.3	1755.7	1933.8	2122.6	2311.1
75	1012.7	1106.9	1203	1306.7	1422.9	1555.7	1707.9	1880	2069.7	2270.6	2470.8
80	1088.8	1187.3	1287.8	1396.7	1519.2	1659.9	1821.5	2004.5	2206.2	2419.4	2631.5
85	1165.9	1268.4	1373.1	1486.9	1615.7	1764.2	1935.3	2129.2	2343	2568.9	2793.3
90	1243.9	1350.3	1458.8	1577.3	1712.2	1868.5	2049.1	2254.2	2480.3	2719.1	2956.3
95	1323	1432.8	1544.9	1667.9	1808.8	1972.8	2162.9	2379.3	2617.9	2870	3120.3

Table A.17 (continued): Variation in enthalpy of saturated LiBr solution as a function of temperature (°C) and LiBr mass fraction

	LiBr mass fraction										
T (°C)	0.25	0.3	0.35	0.4	0.45	0.5	0.55	0.6	0.65	0.7	0.75
100	1402.9	1516	1631.4	1758.7	1905.4	2077.1	2276.9	2504.6	2756	3021.6	3285.4
105	1483.9	1599.8	1718.4	1849.8	2002.1	2181.4	2390.8	2630.1	2894.5	3174	3451.5
110	1565.8	1684.4	1805.8	1941	2098.9	2285.7	2504.8	2755.7	3033.4	3327	3618.7
115	1648.6	1769.7	1893.6	2032.5	2195.7	2390	2618.9	2881.5	3172.6	3480.7	3787
120	1732.4	1855.6	1981.8	2124.1	2292.6	2494.3	2732.9	3007.5	3312.3	3635.1	3956.4
125	1817.1	1942.2	2070.4	2215.9	2389.5	2598.6	2847	3133.7	3452.3	3790.2	4126.7
130	1902.8	2029.5	2159.5	2307.9	2486.4	2702.9	2961.1	3260	3592.8	3945.9	4298.2
135	1989.5	2117.4	2248.9	2400.1	2583.4	2807.2	3075.3	3386.5	3733.6	4102.4	4470.6
140	2077.1	2206.1	2338.8	2492.5	2680.4	2911.4	3189.4	3513.1	3874.7	4259.5	4644.2
145	2165.6	2295.4	2429	2585	2777.5	3015.6	3303.6	3639.9	4016.3	4417.2	4818.7
150	2255	2385.3	2519.7	2677.8	2874.5	3119.8	3417.8	3766.8	4158.2	4575.7	4994.3
155	2345.4	2476	2610.7	2770.7	2971.7	3224	3532	3893.9	4300.5	4734.8	5170.9
160	2436.8	2567.3	2702.2	2863.8	3068.8	3328.1	3646.2	4021.1	4443.1	4894.6	5348.6
165	2529.1	2659.3	2794	2957	3166	3432.2	3760.5	4148.5	4586.1	5055	5527.3
170	2622.3	2751.9	2886.3	3050.5	3263.2	3536.3	3874.7	4276	4729.5	5216.1	5707

A.18. Boiling Temperature of LiBr Water Solution

The correlation for the boiling temperature of saturated LiBr-H_2O solution is given by

$$T(P,X) = \sum_{i=0}^{10} a_i X^i + T_w \sum_{i=0}^{10} b_i X^i \qquad (A.18)$$

where T_w is the saturation temperature of pure water at pressure P, X is the mass fraction of LiBr in the solution, P is the pressure, and T is the boiling temperature of the LiBr-H_2O solution. The constants in the above relation are as follows:

$a_0 = 0$, $a_1 = 16.634856$, $a_2 = -553.38169$, $a_3 = 11228.338$, $a_4 = -110283.9$,
$a_5 = 621094.64$, $a_6 = -2111256.7$, $a_7 = 4385190.1$, $a_8 = -5409811.5$,
$a_9 = 3626674.2$, $a_{10} = -1015305.9$, $b_0 = 1$, $b_1 = -0.068242821$, $b_2 = 5.873619$
$b_3 = -102.78186$, $b_4 = 930.32374$, $b_5 = -4822.394$, $b_6 = 15189.038$,
$b_7 = -29412.863$, $b_8 = 34100.528$, $b_9 = -21671.48$, $b_{10} = 5799.56$

The boiling temperature of saturated LiBr solution is shown in Table A.18 and Fig. A.18 for a temperature range of 10-170 °C and LiBr mass fraction of 0.25-0.75.

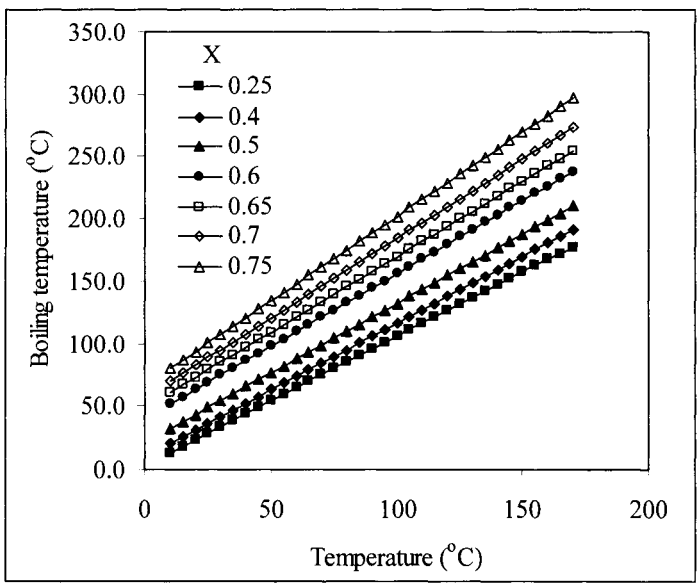

Fig. A.18. Boiling temperature of LiBr solution as a function of temperature and salt concentration

Table A.18: Variation in the boiling temperature of LiBr solution as a function of the salt mass fraction and temperature

	LiBr mass fraction										
T (°C)	0.25	0.3	0.35	0.4	0.45	0.5	0.55	0.6	0.65	0.7	0.75
10	13.5	15.1	17.1	20.0	24.7	31.8	41.0	51.1	60.5	69.4	80.0
15	18.7	20.2	22.3	25.4	30.2	37.4	46.7	56.9	66.5	75.8	86.8
20	23.8	25.4	27.6	30.7	35.6	42.9	52.4	62.7	72.6	82.2	93.5
25	28.9	30.6	32.8	36.1	41.1	48.5	58.1	68.6	78.7	88.6	100.3
30	34.0	35.8	38.1	41.4	46.5	54.1	63.8	74.4	84.7	94.9	107.1
35	39.2	40.9	43.3	46.7	52.0	59.7	69.5	80.3	90.8	101.3	113.9
40	44.3	46.1	48.6	52.1	57.5	65.2	75.2	86.1	96.8	107.7	120.6
45	49.4	51.3	53.8	57.4	62.9	70.8	80.9	91.9	102.9	114.0	127.4
50	54.5	56.5	59.1	62.8	68.4	76.4	86.5	97.8	109.0	120.4	134.2
55	59.7	61.6	64.3	68.1	73.8	81.9	92.2	103.6	115.0	126.8	141.0
60	64.8	66.8	69.6	73.5	79.3	87.5	97.9	109.5	121.1	133.2	147.7
65	69.9	72.0	74.8	78.8	84.7	93.1	103.6	115.3	127.1	139.5	154.5
70	75.0	77.2	80.1	84.2	90.2	98.7	109.3	121.1	133.2	145.9	161.3
75	80.2	82.4	85.3	89.5	95.7	104.2	115.0	127.0	139.3	152.3	168.1
80	85.3	87.5	90.5	94.8	101.1	109.8	120.7	132.8	145.3	158.7	174.8
85	90.4	92.7	95.8	100.2	106.6	115.4	126.4	138.7	151.4	165.0	181.6
90	95.5	97.9	101.0	105.5	112.0	120.9	132.1	144.5	157.4	171.4	188.4

Table A.18 (continued): Variation in the boiling temperature of LiBr solution as a function of the salt mass fraction and temperature

	LiBr mass fraction										
T (°C)	0.25	0.3	0.35	0.4	0.45	0.5	0.55	0.6	0.65	0.7	0.75
95	100.7	103.1	106.3	110.9	117.5	126.5	137.8	150.3	163.5	177.8	195.2
100	105.8	108.2	111.5	116.2	122.9	132.1	143.5	156.2	169.6	184.2	201.9
105	110.9	113.4	116.8	121.6	128.4	137.7	149.2	162.0	175.6	190.5	208.7
110	116.0	118.6	122.0	126.9	133.8	143.2	154.8	167.9	181.7	196.9	215.5
115	121.2	123.8	127.3	132.3	139.3	148.8	160.5	173.7	187.7	203.3	222.3
120	126.3	129.0	132.5	137.6	144.8	154.4	166.2	179.5	193.8	209.7	229.0
125	131.4	134.1	137.8	142.9	150.2	160.0	171.9	185.4	199.9	216.0	235.8
130	136.5	139.3	143.0	148.3	155.7	165.5	177.6	191.2	205.9	222.4	242.6
135	141.7	144.5	148.3	153.6	161.1	171.1	183.3	197.1	212.0	228.8	249.4
140	146.8	149.7	153.5	159.0	166.6	176.7	189.0	202.9	218.1	235.2	256.1
145	151.9	154.8	158.8	164.3	172.0	182.2	194.7	208.8	224.1	241.5	262.9
150	157.0	160.0	164.0	169.7	177.5	187.8	200.4	214.6	230.2	247.9	269.7
155	162.2	165.2	169.3	175.0	183.0	193.4	206.1	220.4	236.2	254.3	276.5
160	167.3	170.4	174.5	180.4	188.4	199.0	211.8	226.3	242.3	260.7	283.2
165	172.4	175.6	179.8	185.7	193.9	204.5	217.5	232.1	248.4	267.0	290.0
170	177.5	180.7	185.0	191.0	199.3	210.1	223.1	238.0	254.4	273.4	296.8

This Page Intentionally Left Blank

Appendix B

Thermodynamic Losses

B.1 Boiling Point Elevation

The correlation for the boiling point elevation of seawater is

$$BPE = A\,X + B\,X^2 + C\,X^3 \qquad (B.1)$$

with

$$A = (8.325\text{x}10^{-2} + 1.883\text{x}10^{-4}\,T + 4.02\text{x}10^{-6}\,T^2)$$

$$B = (-\,7.625\text{x}10^{-4} + 9.02\text{x}10^{-5}\,T - 5.2\text{x}10^{-7}\,T^2)$$

$$C = (1.522\text{x}10^{-4} - 3\text{x}10^{-6}\,T - 3\text{x}10^{-8}\,T^2)$$

where T is the temperature in °C and X is the salt weight percentage. The above equation is valid over the following ranges: $1 \leq X \leq 16\%$, $10 \leq T \leq 180$°C. Variations in the boiling point elevation as a function of the seawater temperature and salinity are given in Table B.1 and Fig. B.1.

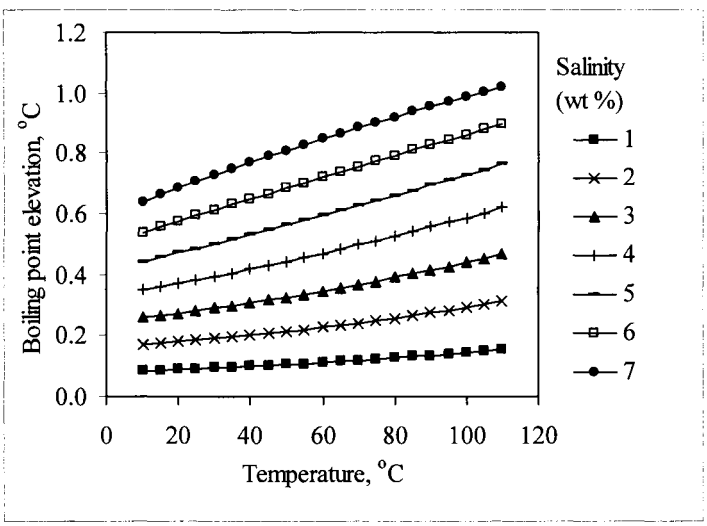

Fig. B.1: Variation in boiling point elevation of seawater as a function of temperature and salinity.

Table B.1: Variation in seawater boiling point elevation (°C) as a function of temperature (°C) and salinity (wt%)

	Salinity (wt%)						
temperature °C	1	2	3	4	5	6	7
10	0.085	0.171	0.258	0.348	0.441	0.538	0.639
15	0.087	0.175	0.266	0.359	0.456	0.556	0.662
20	0.089	0.180	0.273	0.370	0.470	0.575	0.684
25	0.091	0.185	0.281	0.381	0.485	0.593	0.706
30	0.093	0.190	0.290	0.393	0.500	0.612	0.727
35	0.096	0.195	0.298	0.405	0.516	0.630	0.748
40	0.099	0.201	0.307	0.417	0.531	0.648	0.769
45	0.101	0.207	0.316	0.430	0.546	0.666	0.789
50	0.104	0.213	0.326	0.443	0.562	0.684	0.809
55	0.108	0.220	0.336	0.456	0.578	0.703	0.829
60	0.111	0.227	0.346	0.469	0.594	0.721	0.848
65	0.115	0.234	0.357	0.483	0.610	0.739	0.866
70	0.118	0.241	0.368	0.497	0.627	0.756	0.885
75	0.122	0.249	0.379	0.511	0.643	0.774	0.903
80	0.126	0.257	0.391	0.525	0.660	0.792	0.921
85	0.130	0.265	0.402	0.540	0.677	0.810	0.938
90	0.135	0.274	0.415	0.555	0.694	0.828	0.955
95	0.139	0.283	0.427	0.571	0.711	0.845	0.971
100	0.144	0.292	0.440	0.587	0.728	0.863	0.987
105	0.149	0.301	0.453	0.603	0.746	0.880	1.003
110	0.154	0.311	0.467	0.619	0.764	0.898	1.018

B.2 Non-Equilibrium Allowance in MEE

The correlation for the non-equilibrium allowance in the MEE process is developed by Miyatake et al. (1973),

$$(NEA)_j = 33\ (\Delta T_j)^{0.55}/T_{vj} \qquad (B.2)$$

where, $\Delta Tj = T_{j-1} - T_j$, is temperature difference of boiling brine in effects j and j–1, T_{vj} is the vapor temperature in effect j and is given by $T_{vj} = T_j - (BPE)_j$. All temperatures in the above correlation are in °C. Results for the non-equilibrium allowance are shown in Table B.2 and Fig. B.2.

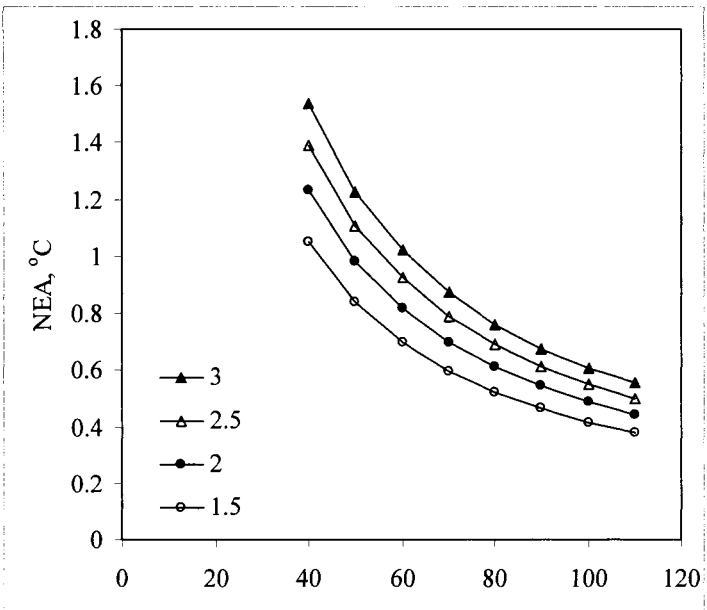

Fig. B.2 Variation in non-equilibrium allowance in MEE as a function of brine temperature and temperature drop per effect for salinity of 40000 ppm

Table B.2: Variation in the non-equilibrium allowance in multiple effect evaporation as a function of effect temperature drop and temperature for a salinity of 40000 ppm.

NEA (°C)	T_j	ΔT	T_{v_j}	BPE (°C)
1.042	40	1.5	39.6	0.417
0.832	50	1.5	49.6	0.443
0.693	60	1.5	59.5	0.469
0.593	70	1.5	69.5	0.497
0.519	80	1.5	79.5	0.525
0.461	90	1.5	89.4	0.555
0.415	100	1.5	99.4	0.587
0.377	110	1.5	109.4	0.619
1.221	40	2	39.6	0.417
0.975	50	2	49.6	0.443
0.812	60	2	59.5	0.469
0.695	70	2	69.5	0.497
0.608	80	2	79.5	0.525
0.540	90	2	89.4	0.555
0.486	100	2	99.4	0.587
0.442	110	2	109.4	0.619
1.380	40	2.5	39.6	0.417
1.102	50	2.5	49.6	0.443
0.918	60	2.5	59.5	0.469
0.786	70	2.5	69.5	0.497
0.687	80	2.5	79.5	0.525
0.611	90	2.5	89.4	0.555
0.549	100	2.5	99.4	0.587
0.499	110	2.5	109.4	0.619
1.557	40	3	39.6	0.417
1.232	50	3	49.6	0.443
1.020	60	3	59.5	0.469
0.871	70	3	69.5	0.497
0.761	80	3	79.5	0.525
0.675	90	3	89.4	0.555
0.607	100	3	99.4	0.587
0.551	110	3	109.4	0.619

B.3 Non-Equilibrium Allowance in MSF

Lior (1986) developed correlations for the non-equilibrium allowance for the MSF system. The following two equations give values for NEA as a function of the brine temperature, gate height, the brine flow rate per unit length of the chamber width, and the stage temperature drop;

$$(NEA)_{10} = (0.9784)^{Ti}\,(15.7378)^{H}\,(1.3777)^{V_b x 10^{-6}} \qquad \text{(B.3a)}$$

and

$$NEA = (NEA_{10}/(0.5\Delta T + NEA_{10})^{0.3281L}\,(0.5\,\Delta T + NEA_{10}) \qquad \text{(B.3b)}$$

Eq. B.3a is valid for 10 ft stage length and Eq. B.3b is applicable for stages of any other lengths. In the above equation, T_i is the stage temperature in °C, H is the height of the brine pool in m, V_b is the brine flow rate per unit length of the chamber width in kg/(m s), and ΔT is the stage temperature drop in °C Results for the equations B.3a and B.3b are shown in Fig. B.3 and Table B.3.

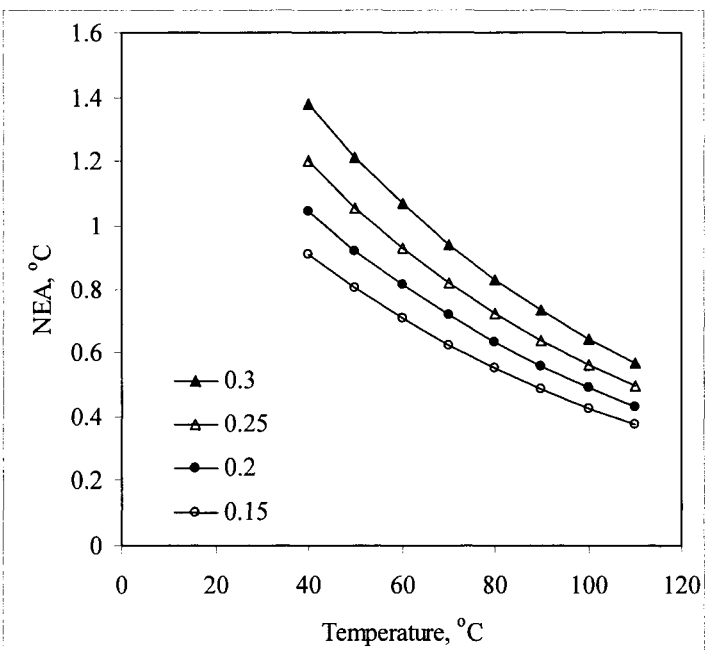

Fig. B.3 Variation in non-equilibrium allowance in MSF as a function of brine temperature and brine height for brine weir load of 180 kg/m/s and stage length = 10 ft.

Table B.3: Variations in non-equilibrium allowance for MSF as a function of flashing temperature and brine height for a weir load of 180 kg/m s and stage length equal to 10 ft.

NEA (°C)	T_j (°C)	H (m)	NEA (°C)	T_j (°C)	H (m)
0.63	40	0.15	0.83	40	0.25
0.51	50	0.15	0.67	50	0.25
0.41	60	0.15	0.54	60	0.25
0.33	70	0.15	0.43	70	0.25
0.26	80	0.15	0.35	80	0.25
0.21	90	0.15	0.28	90	0.25
0.17	100	0.15	0.22	100	0.25
0.14	110	0.15	0.18	110	0.25
0.72	40	0.2	0.95	40	0.3
0.58	50	0.2	0.77	50	0.3
0.47	60	0.2	0.62	60	0.3
0.38	70	0.2	0.50	70	0.3
0.30	80	0.2	0.40	80	0.3
0.24	90	0.2	0.32	90	0.3
0.20	100	0.2	0.26	100	0.3
0.16	110	0.2	0.21	110	0.3

B.4 Demister Pressure Drop

The correlation for pressure drop in the demister, ΔP_p, is developed by El-Dessouky et al. (2000) for industrial type wire pads. The ranges of the experimental variables were V (0.98-7.5 m/s), ρ_p (80.317-208.16 kg/m^3), L (100-200 mm), δ_w (0.2-.32 mm), and d_d (1-5 mm). This correlation is given by

$$\Delta P_p = 3.88178\,(\rho_p)^{0.375798}(V)^{0.81317}(\delta_w)^{-1.56114147} \tag{B.4}$$

where ΔP_p is the demister pressure drop in Pa/m, δ_w is the wire diameter in mm, d_d is the diameter of entrained droplets in mm, L is the mesh pad thickness in mm, V is the vapor velocity in the demister in m/s, and ρ is the demister density in kg/m^3. In Eq. B.4 the subscript p denotes the demister. Results for the demister pressure drop is shown in Table B.4. Figures illustrating the demister pressure are given in Chapter 9.

Table B.4: Variations in the demister pressure drop as a function of the vapor velocity, packing density, and wire diameter.

Δp (Pa/m)	V (m/s)	ρp (kg/m3)	δ_w (m)	Δp (Pa/m)	V (m/s)	ρp (kg/m3)	δ_w (m)
190.1495	1.37	80.317	0.28	799.5571	5.16	208.16	0.28
299.9815	2.4	80.317	0.28	832.1666	5.42	208.16	0.28
370.3531	3.11	80.317	0.28	429.5316	1.36	176.35	0.2
419.028	3.62	80.317	0.28	597.2926	2.04	176.35	0.2
456.3063	4.02	80.317	0.28	656.1643	2.29	176.35	0.2
594.874	5.57	80.317	0.28	342.3253	1.46	176.35	0.24
689.6065	6.68	80.317	0.28	434.9566	1.96	176.35	0.24
527.0877	4.8	80.317	0.28	581.3096	2.8	176.35	0.24
631.9565	6	80.317	0.28	672.578	3.35	176.35	0.24
352.5772	2.26	140.6	0.28	769.0008	3.95	176.35	0.24
441.4914	2.98	140.6	0.28	839.5147	4.4	176.35	0.24
520.6471	3.65	140.6	0.28	931.4795	5	176.35	0.24
590.3651	4.26	140.6	0.28	885.7715	4.7	176.35	0.24
673.5824	5.01	140.6	0.28	383.9096	2.26	176.35	0.28
751.298	5.73	140.6	0.28	480.7253	2.98	176.35	0.28
804.1878	6.23	140.6	0.28	566.9154	3.65	176.35	0.28
327.6714	1.86	176.35	0.28	642.8291	4.26	176.35	0.28
434.2842	2.63	176.35	0.28	733.4416	5.01	176.35	0.28
517.1443	3.26	176.35	0.28	818.0635	5.73	176.35	0.28
644.0559	4.27	176.35	0.28	875.6535	6.23	176.35	0.28
720.3196	4.9	176.35	0.28	243.6977	1.67	176.35	0.32
799.4394	5.57	176.35	0.28	301.5393	2.17	176.35	0.32
829.6542	5.83	176.35	0.28	374.2175	2.83	176.35	0.32
333.4171	1.76	208.16	0.28	471.4877	3.76	176.35	0.32
452.1815	2.56	208.16	0.28	546.6402	4.51	176.35	0.32
543.5242	3.21	208.16	0.28	601.2238	5.07	176.35	0.32
676.3193	4.2	208.16	0.28	659.4141	5.68	176.35	0.32
761.546	4.86	208.16	0.28	761.5104	6.78	176.35	0.32
772.7173	2.8	176.35	0.2	721.0738	6.34	176.35	0.32
848.1905	3.14	176.35	0.2	809.5738	7.31	176.35	0.32
935.0569	3.54	176.35	0.2	687.5985	5.98	176.35	0.32
965.0183	3.68	176.35	0.2	790.6104	7.1	176.35	0.32

B.5 Pressure Drop in Connecting Lines

The pressure drop in the lines connecting the vapor space in effect i and the evaporator tubes of the next effect is calculated from the Unwin formula, ORNL (1967),

$$\Delta P = \frac{0.0001306\ M^2\ L\ (1+\frac{3.6}{\delta_i})}{\rho_v \delta_i^5} \tag{B.5}$$

where M is the mass flow rate of the vapor stream (kg/s), L is the tube length (m), δ_i is the tube inner diameter (m), ρ_v is the vapor density (kg/m^3), and ΔP is the pressure drop (Pa/m). Results for the pressure drop in connecting lines are given in Table B.5 and Fig. B.5.

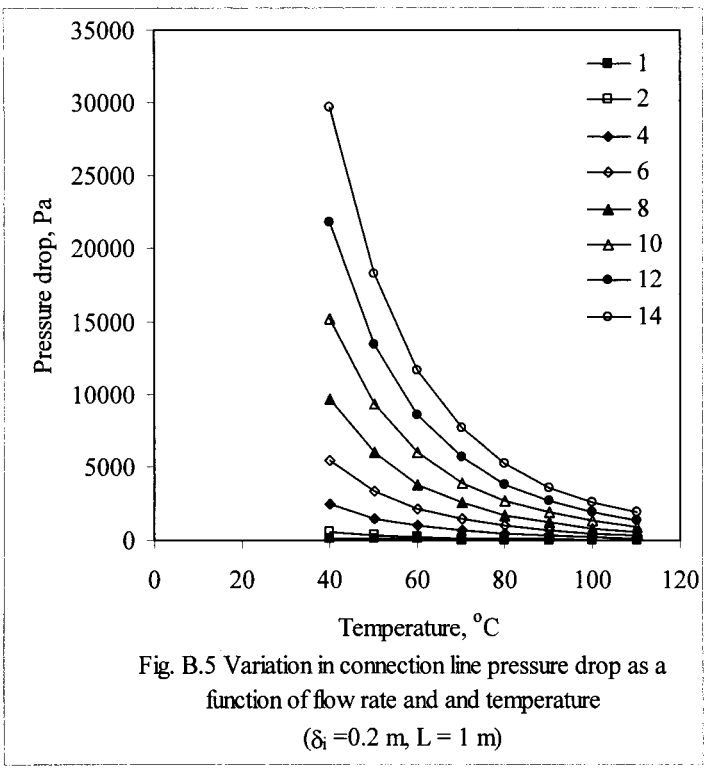

Fig. B.5 Variation in connection line pressure drop as a function of flow rate and and temperature (δ_i =0.2 m, L = 1 m)

Table B.5: Variation in connecting line pressure drop as a function of temperature and flow rate for L = 1 m and δ_i = 0.2 m.

T (°C)	ΔP (Pa/m)	M (kg/s)	ρ_v (kg/m^3)
40	151.3807	1	0.051224324
50	93.28704	1	0.083123816
60	59.47389	1	0.13038284
70	39.09619	1	0.198340913
80	26.42084	1	0.293494667
90	18.3064	1	0.423588291
100	12.97389	1	0.597691043
110	9.384879	1	0.826262685
40	605.5229	2	0.051224324
50	373.1482	2	0.083123816
60	237.8956	2	0.13038284
70	156.3848	2	0.198340913
80	105.6834	2	0.293494667
90	73.22558	2	0.423588291
100	51.89554	2	0.597691043
110	37.53951	2	0.826262685
40	2422.092	4	0.051224324
50	1492.593	4	0.083123816
60	951.5823	4	0.13038284
70	625.5391	4	0.198340913
80	422.7334	4	0.293494667
90	292.9023	4	0.423588291
100	207.5822	4	0.597691043
110	150.1581	4	0.826262685
40	5449.706	6	0.051224324
50	3358.334	6	0.083123816
60	2141.06	6	0.13038284
70	1407.463	6	0.198340913
80	951.1502	6	0.293494667
90	659.0303	6	0.423588291
100	467.0599	6	0.597691043
110	337.8556	6	0.826262685
40	9688.366	8	0.051224324
50	5970.371	8	0.083123816
60	3806.329	8	0.13038284
70	2502.156	8	0.198340913
80	1690.934	8	0.293494667
90	1171.609	8	0.423588291
100	830.3287	8	0.597691043
110	600.6322	8	0.826262685

Table B.5 (Continued): Variation in connecting line pressure drop as a function of temperature and flow rate for L = 1 m and δ_i = 0.2 m.

T (°C)	ΔP (Pa/m)	M (kg/s)	ρ_v (kg/m^3)
40	15138.07	10	0.051224324
50	9328.704	10	0.083123816
60	5947.389	10	0.13038284
70	3909.619	10	0.198340913
80	2642.084	10	0.293494667
90	1830.64	10	0.423588291
100	1297.389	10	0.597691043
110	938.4879	10	0.826262685
40	21798.82	12	0.051224324
50	13433.33	12	0.083123816
60	8564.241	12	0.13038284
70	5629.852	12	0.198340913
80	3804.601	12	0.293494667
90	2636.121	12	0.423588291
100	1868.239	12	0.597691043
110	1351.423	12	0.826262685
40	29670.62	14	0.051224324
50	18284.26	14	0.083123816
60	11656.88	14	0.13038284
70	7662.854	14	0.198340913
80	5178.484	14	0.293494667
90	3588.054	14	0.423588291
100	2542.882	14	0.597691043
110	1839.436	14	0.826262685

B.6 Gravitational Pressure Drop

The gravitational pressure drop during condensation inside the evaporator tubes is given by

$$\Delta P = \left(\rho_v \alpha + (1-\alpha)\rho_\ell\right) g\, L \sin(\theta) \tag{B.6}$$

where ΔP is the pressure drop in Pa, g is the gravitational acceleration (m/s^2), L is length of the evaporator tubes (m), and θ is the inclination angle. The expression for α is given by Zivi (1964), $\alpha = \dfrac{1}{\left(1 + \dfrac{1-\chi}{\chi}\left(\dfrac{\rho_v}{\rho_\ell}\right)^{0.5}\right)}$, where χ is the vapor mass fraction, which is greater than zero and less than 1. In Eq. B.6, ρ_v and ρ_ℓ are the density of vapor and liquid streams at saturation conditions and are given in (kg/m^3). Results for the above losses are given in Table B.6 and Fig. B.6.

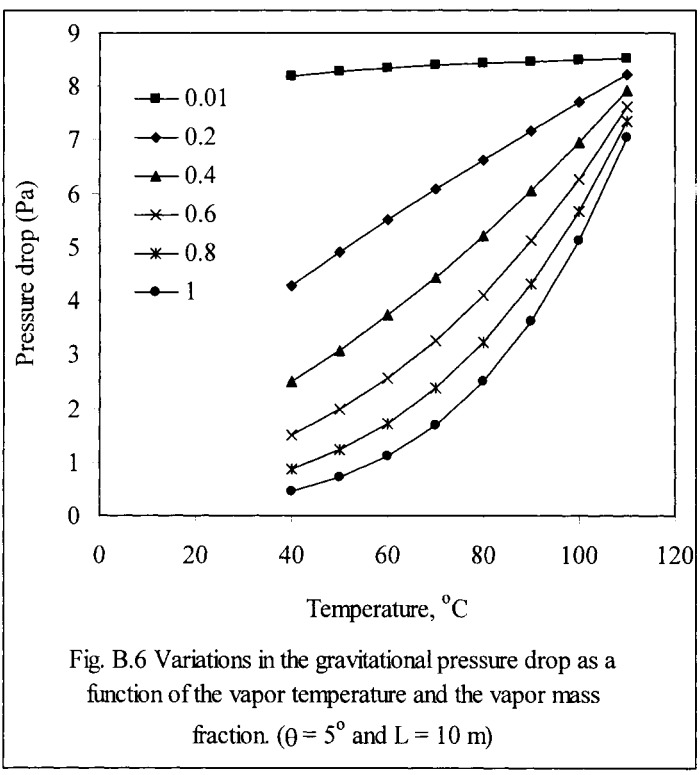

Fig. B.6 Variations in the gravitational pressure drop as a function of the vapor temperature and the vapor mass fraction. ($\theta = 5^\circ$ and L = 10 m)

Table B.6: Variation in gravitational pressure drop as a function of temperature and vapor mass fraction for $\theta = 5^{o}$ and L = 10 m.

ΔP (Pa)	T (^{o}C)	χ	ρ_{ℓ} (kg/m^3)	ρ_V (kg/m^3)
3522.797	40	0.01	992.19	0.051224
4016.468	50	0.01	988.00	0.083124
4473.981	60	0.01	983.14	0.130383
4886.44	70	0.01	977.68	0.198341
5249.686	80	0.01	971.68	0.293495
5563.216	90	0.01	965.18	0.423588
5829.014	100	0.01	958.23	0.597691
6050.516	110	0.01	950.84	0.826263
237.1867	40	0.2	992.19	0.051224
299.3431	50	0.2	988.00	0.083124
370.8429	60	0.2	983.14	0.130383
451.7166	70	0.2	977.68	0.198341
541.7984	80	0.2	971.68	0.293495
640.7363	90	0.2	965.18	0.423588
748.0056	100	0.2	958.23	0.597691
862.9278	110	0.2	950.84	0.826263
90.79624	40	0.4	992.19	0.051224
115.2305	50	0.4	988.00	0.083124
143.686	60	0.4	983.14	0.130383
176.336	70	0.4	977.68	0.198341
213.3048	80	0.4	971.68	0.293495
254.669	90	0.4	965.18	0.423588
300.4589	100	0.4	958.23	0.597691
350.6601	110	0.4	950.84	0.826263

Table B.6 (Continued): Variation in gravitational pressure drop as a function of temperature and vapor mass fraction for $\theta = 5^{o}$ and L = 10 m.

ΔP (Pa)	T (^{o}C)	χ	ρ_{ℓ} (kg/m^3)	ρ_V (kg/m^3)
40.830	40	0.6	992.19	0.051224
51.987	50	0.6	988.00	0.083124
65.076	60	0.6	983.14	0.130383
80.222	70	0.6	977.68	0.198341
97.539	80	0.6	971.68	0.293495
117.127	90	0.6	965.18	0.423588
139.076	100	0.6	958.23	0.597691
163.466	110	0.6	950.84	0.826263
15.630	40	0.8	992.19	0.051224
20.012	50	0.8	988.00	0.083124
25.214	60	0.8	983.14	0.130383
31.316	70	0.8	977.68	0.198341
38.401	80	0.8	971.68	0.293495
46.553	90	0.8	965.18	0.423588
55.864	100	0.8	958.23	0.597691
66.426	110	0.8	950.84	0.826263
1.052	40	0.99	992.19	0.051224
1.492	50	0.99	988.00	0.083124
2.090	60	0.99	983.14	0.130383
2.895	70	0.99	977.68	0.198341
3.963	80	0.99	971.68	0.293495
5.361	90	0.99	965.18	0.423588
7.168	100	0.99	958.23	0.597691
9.473	110	0.99	950.84	0.826263

B.7 Acceleration Pressure Drop

The acceleration pressure drop during condensation inside the evaporator tubes is calculated from the following relation

$$\Delta P = \frac{M^2}{A^2}\left(\frac{\chi_1^2}{\alpha_1 \rho_{v_1}} + \frac{(1-\chi_1)^2}{(1-\alpha_1)\rho_{\ell_1}} - \frac{\chi_2^2}{\alpha_2 \rho_{v_2}} - \frac{(1-\chi_2)^2}{(1-\alpha_2)\rho_{\ell_2}}\right) \tag{B.7}$$

where ΔP is the pressure drop in Pa, M is the mass flow rate in kg/s, A is the cross section area in m^2, ρ_v is the vapor density in kg/m^3, ρ_ℓ is the liquid density in kg/m^3, χ is the vapor phase mass fraction, α is $\alpha = \dfrac{1}{\left(1 + \dfrac{1-\chi}{\chi}\left(\dfrac{\rho_v}{\rho_\ell}\right)^{0.5}\right)}$. The subscripts 1 and 2 refer to the inlet and outlet conditions. Results for the above correlation are shown in Table B.7 and Fig. B.7.

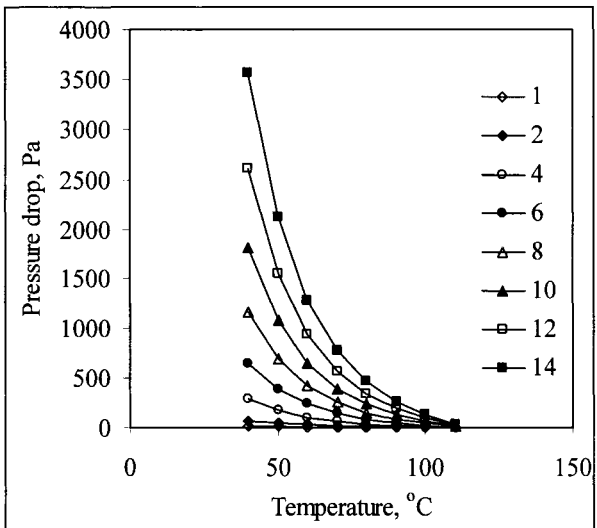

Fig. B.7. Variation in the acceleration pressure drop as a function of temperature and flow rate. ($A = 1\ m^2$, $\chi_1 = 0.99$, $\chi_2 = 0.01$)

Table B.7: Variations in the acceleration pressure drop as a function of the mass flow rate and temperature for a cross section area of 1 m2 and vapor mass fractions of 0.01 and 0.99.

T (°C)	ΔP (Pa)	M (kg/s)	ρ_ℓ (kg/m^3)	ρ_V (kg/m^3)	α_1	α_2
40	19.13	1	992.19	0.05	0.9573	0.0023
50	11.79	1	988.00	0.08	0.9662	0.0029
60	7.52	1	983.14	0.13	0.9728	0.0036
70	4.94	1	977.68	0.20	0.9778	0.0045
80	3.34	1	971.68	0.29	0.9817	0.0054
90	2.31	1	965.18	0.42	0.9847	0.0065
100	1.64	1	958.23	0.60	0.9871	0.0077
110	1.19	1	950.84	0.83	0.9890	0.0091
40	76.52	2	992.19	0.05	0.9573	0.0023
50	47.15	2	988.00	0.08	0.9662	0.0029
60	30.06	2	983.14	0.13	0.9728	0.0036
70	19.76	2	977.68	0.20	0.9778	0.0045
80	13.35	2	971.68	0.29	0.9817	0.0054
90	9.25	2	965.18	0.42	0.9847	0.0065
100	6.55	2	958.23	0.60	0.9871	0.0077
110	4.74	2	950.84	0.83	0.9890	0.0091
40	306.09	4	992.19	0.05	0.9573	0.0023
50	188.62	4	988.00	0.08	0.9662	0.0029
60	120.25	4	983.14	0.13	0.9728	0.0036
70	79.04	4	977.68	0.20	0.9778	0.0045
80	53.41	4	971.68	0.29	0.9817	0.0054
90	37.00	4	965.18	0.42	0.9847	0.0065
100	26.22	4	958.23	0.60	0.9871	0.0077
110	18.96	4	950.84	0.83	0.9890	0.0091
40	688.70	6	992.19	0.05	0.9573	0.0023
50	424.39	6	988.00	0.08	0.9662	0.0029
60	270.55	6	983.14	0.13	0.9728	0.0036
70	177.84	6	977.68	0.20	0.9778	0.0045
80	120.17	6	971.68	0.29	0.9817	0.0054
90	83.25	6	965.18	0.42	0.9847	0.0065
100	58.99	6	958.23	0.60	0.9871	0.0077
110	42.66	6	950.84	0.83	0.9890	0.0091
40	1224.36	8	992.19	0.05	0.9573	0.0023
50	754.47	8	988.00	0.08	0.9662	0.0029
60	480.98	8	983.14	0.13	0.9728	0.0036
70	316.16	8	977.68	0.20	0.9778	0.0045
80	213.64	8	971.68	0.29	0.9817	0.0054
90	148.01	8	965.18	0.42	0.9847	0.0065
100	104.87	8	958.23	0.60	0.9871	0.0077
110	75.85	8	950.84	0.83	0.9890	0.0091

Table B.7 (continued): Variations in the acceleration pressure drop as a function of the mass flow rate and temperature for a cross section area of 1 m^2 and vapor mass fractions of 0.01 and 0.99.

T (°C)	ΔP (Pa)	M (kg/s)	ρ_ℓ (kg/m^3)	ρ_v (kg/m^3)	α_1	α_2
40	1913.06	10	992.19	0.05	0.9573	0.0023
50	1178.87	10	988.00	0.08	0.9662	0.0029
60	751.53	10	983.14	0.13	0.9728	0.0036
70	494.00	10	977.68	0.20	0.9778	0.0045
80	333.81	10	971.68	0.29	0.9817	0.0054
90	231.26	10	965.18	0.42	0.9847	0.0065
100	163.87	10	958.23	0.60	0.9871	0.0077
110	118.51	10	950.84	0.83	0.9890	0.0091
40	2754.80	12	992.19	0.05	0.9573	0.0023
50	1697.57	12	988.00	0.08	0.9662	0.0029
60	1082.21	12	983.14	0.13	0.9728	0.0036
70	711.36	12	977.68	0.20	0.9778	0.0045
80	480.69	12	971.68	0.29	0.9817	0.0054
90	333.01	12	965.18	0.42	0.9847	0.0065
100	235.97	12	958.23	0.60	0.9871	0.0077
110	170.65	12	950.84	0.83	0.9890	0.0091
40	3749.59	14	992.19	0.05	0.9573	0.0023
50	2310.58	14	988.00	0.08	0.9662	0.0029
60	1473.01	14	983.14	0.13	0.9728	0.0036
70	968.24	14	977.68	0.20	0.9778	0.0045
80	654.27	14	971.68	0.29	0.9817	0.0054
90	453.27	14	965.18	0.42	0.9847	0.0065
100	321.18	14	958.23	0.60	0.9871	0.0077
110	232.28	14	950.84	0.83	0.9890	0.0091

References

El-Dessouky, H.T., Alatiqi, I.M., **Ettouney, H.M.**, and Al-Deffeeri, N.S., Performance of wire mesh mist eliminator, Chem. Eng. & Proc., **39**(2000)129-139.

Lior, N., Formulas for calculating the approach to equilibrium in open channel flash evaporators for saline water, Desalination, **60**(1986)223.

Miyatake, O., Murakami, K., Kawata, Y., and Fujii, Fundamental Experiments with Flash Evaporation, Heat Transfer Jpn. Res., **2**(1973)89-100.

Oak Ridge National Laboratory (ORNL), United States Department of the Interior, Research and Development Progress Report No. 315, December 1967.

Zivi, S.M., Estimation of steady-state steam void fraction by means of the principle of minimum entropy production, Trans. ASME, J. of Heat Transfer, **86**(1964), 247-252.

This Page Intentionally Left Blank

Appendix C

Heat Transfer Coefficients

C.1 Falling Film on the Tube Outside Surface

The heat transfer coefficient of boiling thin film of water flowing over the outside surface of smooth horizontal tubes was developed by Han and Fletcher (1985),

$$h = 0.0004\ (\rho^2\ g\ k^3/\mu^2)^{1/3}\ Re^{0.2}\ Pr^{0.65}\ q^{0.4} \qquad (C.1)$$

The relationship is valid over the following parameter range; $770 \leq Re \leq 7000$, $1.3 \leq Pr \leq 3.6$, $30 \leq q \leq 80$ kW/m^2, and $49 \leq T \leq 127$ °C. In the above equation Re and Pr are Reynolds and Prandtl numbers respectively, q, is the heat flux, μ is the viscosity, ρ is the density and k is the thermal conductivity of the fluid. Table C.1 and Fig. C.1 show variations in the heat transfer coefficient as a function of the system temperature and the heat flux.

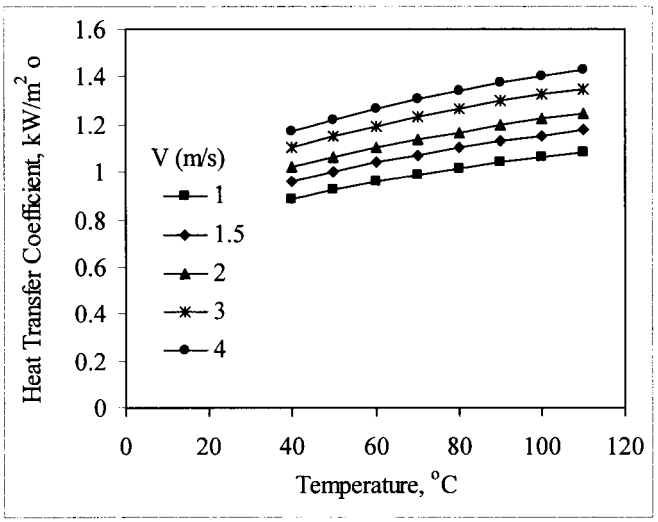

Fig. C.1. Variation in the heat transfer coefficient for boiling falling film

Table C.1: The heat transfer coefficient for boiling falling film for δ_o = 0.03 m, δ_i = 0.025 m, q = 80 kW/m^2, and X = 40000 ppm.

T (°C)	h (kW/m^2 °C)	V (m/s)	Re	Pr	k (kW/m °C)	μ (kg/m s)	Cp (kJ/kg °C)	ρ (kg/m^3)
40	0.89	1	42784.24	4.54	6.28E-04	7.16E-04	3.98	1021.37
50	0.92	1	50750.40	3.75	6.39E-04	6.01E-04	3.99	1017.07
60	0.96	1	59113.56	3.16	6.48E-04	5.14E-04	3.99	1012.24
70	0.99	1	67786.84	2.71	6.57E-04	4.46E-04	4.00	1006.89
80	1.02	1	76688.39	2.36	6.64E-04	3.92E-04	4.00	1001.06
90	1.04	1	85742.46	2.08	6.70E-04	3.48E-04	4.01	994.75
100	1.06	1	94879.95	1.86	6.74E-04	3.12E-04	4.02	987.99
110	1.08	1	104038.65	1.68	6.78E-04	2.83E-04	4.03	980.79
40	0.96	1.5	64176.36	4.54	6.28E-04	7.16E-04	3.98	1021.37
50	1.00	1.5	76125.61	3.75	6.39E-04	6.01E-04	3.99	1017.07
60	1.04	1.5	88670.34	3.16	6.48E-04	5.14E-04	3.99	1012.24
70	1.07	1.5	101680.26	2.71	6.57E-04	4.46E-04	4.00	1006.89
80	1.10	1.5	115032.59	2.36	6.64E-04	3.92E-04	4.00	1001.06
90	1.13	1.5	128613.69	2.08	6.70E-04	3.48E-04	4.01	994.75
100	1.15	1.5	142319.92	1.86	6.74E-04	3.12E-04	4.02	987.99
110	1.18	1.5	156057.97	1.68	6.78E-04	2.83E-04	4.03	980.79
40	1.02	2	85568.48	4.54	6.28E-04	7.16E-04	3.98	1021.37
50	1.06	2	101500.81	3.75	6.39E-04	6.01E-04	3.99	1017.07
60	1.10	2	118227.11	3.16	6.48E-04	5.14E-04	3.99	1012.24
70	1.14	2	135573.68	2.71	6.57E-04	4.46E-04	4.00	1006.89
80	1.17	2	153376.79	2.36	6.64E-04	3.92E-04	4.00	1001.06
90	1.20	2	171484.92	2.08	6.70E-04	3.48E-04	4.01	994.75
100	1.22	2	189759.90	1.86	6.74E-04	3.12E-04	4.02	987.99
110	1.25	2	208077.30	1.68	6.78E-04	2.83E-04	4.03	980.79
40	1.10	3	128352.72	4.54	6.28E-04	7.16E-04	3.98	1021.37
50	1.15	3	152251.21	3.75	6.39E-04	6.01E-04	3.99	1017.07
60	1.19	3	177340.67	3.16	6.48E-04	5.14E-04	3.99	1012.24
70	1.23	3	203360.52	2.71	6.57E-04	4.46E-04	4.00	1006.89
80	1.27	3	230065.18	2.36	6.64E-04	3.92E-04	4.00	1001.06
90	1.30	3	257227.37	2.08	6.70E-04	3.48E-04	4.01	994.75
100	1.33	3	284639.85	1.86	6.74E-04	3.12E-04	4.02	987.99
110	1.35	3	312115.95	1.68	6.78E-04	2.83E-04	4.03	980.79
40	1.17	4	171136.95	4.54	6.28E-04	7.16E-04	3.98	1021.37
50	1.22	4	203001.62	3.75	6.39E-04	6.01E-04	3.99	1017.07
60	1.26	4	236454.23	3.16	6.48E-04	5.14E-04	3.99	1012.24
70	1.30	4	271147.36	2.71	6.57E-04	4.46E-04	4.00	1006.89
80	1.34	4	306753.57	2.36	6.64E-04	3.92E-04	4.00	1001.06
90	1.37	4	342969.83	2.08	6.70E-04	3.48E-04	4.01	994.75
100	1.40	4	379519.80	1.86	6.74E-04	3.12E-04	4.02	987.99
110	1.43	4	416154.60	1.68	6.78E-04	2.83E-04	4.03	980.79

C.2 *Vapor Condensation Inside Tubes*

The heat transfer coefficient for vapor condensation inside horizontal tubes was developed by Shah (1978).

$$h/h_u = 1 + 3.8 / Z^{0.95} \qquad (C.2)$$

where $Z = ((1/\chi) - 1)^{0.8} Pr^{0.4}$, $h_u = h_\ell (1 - \chi)^{0.8}$, $h_\ell = 0.023 Re^{0.8} Pr^{0.4} (k_\ell/\delta_i)$, χ is the vapor phase mass fraction and the subscripts i, ℓ, and u denotes the tube inside, the liquid phase, and the local superficial value. The above correlation is valid over the following ranges: $2.8 \leq \delta_i \leq 40$ mm, $21 \leq T \leq 355$ °C, $0 \leq \chi \leq 1$, $0.158 \leq q \leq 16000$ kW/m^2, $11 \leq G \leq 4000$ kg/m^2 s, $0.7 \leq P \leq 1$ bar, $0.0019 \leq Pr \leq 0.82$, $350 \leq Re \leq 100000$. Table C.2 and Fig. C.2 show variations in the heat transfer coefficient as a function of the system temperature and vapor fraction.

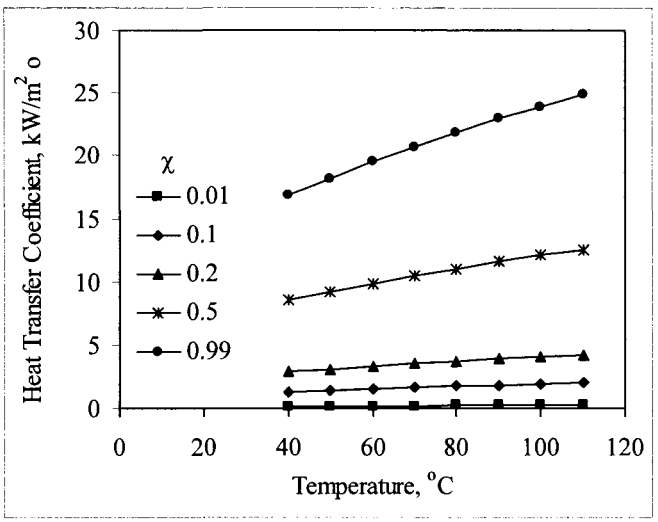

Fig. C.2. Variation in the heat transfer coefficient for vapor condensation inside the tubes

Table C.2: The heat transfer coefficient for vapor condensation inside the tubes, for δ_o = 0.03 m, δ_i = 0.025 m, and X = 40000 ppm.

T (°C)	h (kW/m^2 °C)	χ	Re	Pr	k (kW/m °C)	μ (kg/m s)	Cp (kJ/kg °C)	ρ (kg/m^3)
40	0.15	0.01	427.84	4.54	6.28E-04	7.16E-04	3.98	1021.37
50	0.16	0.01	507.50	3.75	6.39E-04	6.01E-04	3.99	1017.07
60	0.17	0.01	591.14	3.16	6.48E-04	5.14E-04	3.99	1012.24
70	0.18	0.01	677.87	2.71	6.57E-04	4.46E-04	4.00	1006.89
80	0.19	0.01	766.88	2.36	6.64E-04	3.92E-04	4.00	1001.06
90	0.20	0.01	857.42	2.08	6.70E-04	3.48E-04	4.01	994.75
100	0.21	0.01	948.80	1.86	6.74E-04	3.12E-04	4.02	987.99
110	0.22	0.01	1040.39	1.68	6.78E-04	2.83E-04	4.03	980.79
40	1.34	0.1	4278.42	4.54	6.28E-04	7.16E-04	3.98	1021.37
50	1.45	0.1	5075.04	3.75	6.39E-04	6.01E-04	3.99	1017.07
60	1.55	0.1	5911.36	3.16	6.48E-04	5.14E-04	3.99	1012.24
70	1.65	0.1	6778.68	2.71	6.57E-04	4.46E-04	4.00	1006.89
80	1.74	0.1	7668.84	2.36	6.64E-04	3.92E-04	4.00	1001.06
90	1.83	0.1	8574.25	2.08	6.70E-04	3.48E-04	4.01	994.75
100	1.91	0.1	9487.99	1.86	6.74E-04	3.12E-04	4.02	987.99
110	1.98	0.1	10403.86	1.68	6.78E-04	2.83E-04	4.03	980.79
40	2.88	0.2	8556.85	4.54	6.28E-04	7.16E-04	3.98	1021.37
50	3.11	0.2	10150.08	3.75	6.39E-04	6.01E-04	3.99	1017.07
60	3.33	0.2	11822.71	3.16	6.48E-04	5.14E-04	3.99	1012.24
70	3.54	0.2	13557.37	2.71	6.57E-04	4.46E-04	4.00	1006.89
80	3.74	0.2	15337.68	2.36	6.64E-04	3.92E-04	4.00	1001.06
90	3.92	0.2	17148.49	2.08	6.70E-04	3.48E-04	4.01	994.75
100	4.09	0.2	18975.99	1.86	6.74E-04	3.12E-04	4.02	987.99
110	4.25	0.2	20807.73	1.68	6.78E-04	2.83E-04	4.03	980.79
40	8.49	0.5	21392.12	4.54	6.28E-04	7.16E-04	3.98	1021.37
50	9.18	0.5	25375.20	3.75	6.39E-04	6.01E-04	3.99	1017.07
60	9.83	0.5	29556.78	3.16	6.48E-04	5.14E-04	3.99	1012.24
70	10.45	0.5	33893.42	2.71	6.57E-04	4.46E-04	4.00	1006.89
80	11.03	0.5	38344.20	2.36	6.64E-04	3.92E-04	4.00	1001.06
90	11.57	0.5	42871.23	2.08	6.70E-04	3.48E-04	4.01	994.75
100	12.08	0.5	47439.97	1.86	6.74E-04	3.12E-04	4.02	987.99
110	12.55	0.5	52019.32	1.68	6.78E-04	2.83E-04	4.03	980.79
40	16.82	0.99	42356.40	4.54	6.28E-04	7.16E-04	3.98	1021.37
50	18.18	0.99	50242.90	3.75	6.39E-04	6.01E-04	3.99	1017.07
60	19.47	0.99	58522.42	3.16	6.48E-04	5.14E-04	3.99	1012.24
70	20.69	0.99	67108.97	2.71	6.57E-04	4.46E-04	4.00	1006.89
80	21.84	0.99	75921.51	2.36	6.64E-04	3.92E-04	4.00	1001.06
90	22.92	0.99	84885.03	2.08	6.70E-04	3.48E-04	4.01	994.75
100	23.93	0.99	93931.15	1.86	6.74E-04	3.12E-04	4.02	987.99
110	24.86	0.99	102998.26	1.68	6.78E-04	2.83E-04	4.03	980.79

C.3 Seawater Flowing Inside Tubes

The heat transfer coefficient for seawater inside the tubes was developed for desalination plants by Wangnick (1995).

$$h = (3293.5+T(84.24-0.1714\ T) - x\ (8.471+0.1161\ x + 0.2716\ T))/((\delta_i/0.017272)^{0.2}) ((0.656\ V)^{0.8})\ (\delta_i/\delta_o) \quad (C.3)$$

where x is the salt concentration in weight percent, T is the temperature, and δ_i and δ_o are the inside and the outside tube diameter respectively. Table C.3 and Fig. C.3 show variations in the heat transfer coefficient as a function of the system temperature and the velocity. Table C.3 includes also values of the heat transfer coefficient as predicted by the Dittus-Bolter equation. It should be noted that values for Reynolds number, Prandtl number, and other physical properties are the same as those given in Table C.1.

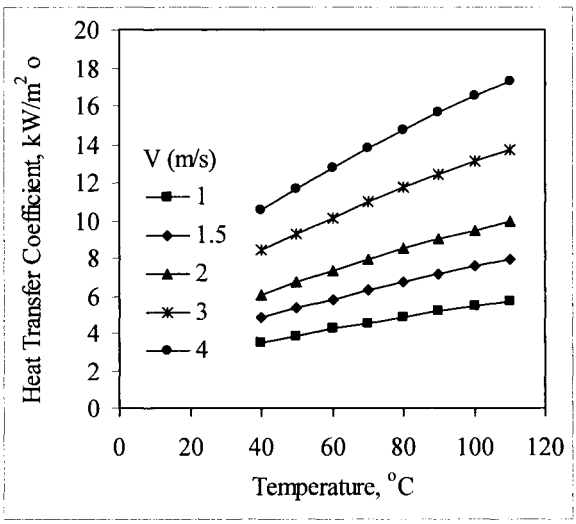

Fig. C.3. Variation in the heat transfer coefficient for seawater flowing inside the tubes

Table C.3: The heat transfer coefficient for seawater flowing inside the tubes, for $\delta_o = 0.03$ m, $\delta_i = 0.025$ m, and X = 40000 ppm.

T (°C)	h (Eq. C.3) (kW/m^2 °C)	h (Dittus-Bolter) (kW/m^2 °C)	V (m/s)
40	3.49	4.19	1
50	3.86	4.58	1
60	4.21	4.97	1
70	4.55	5.33	1
80	4.87	5.68	1
90	5.17	6.01	1
100	5.45	6.32	1
110	5.71	6.62	1
40	4.82	5.79	1.5
50	5.34	6.34	1.5
60	5.83	6.87	1.5
70	6.29	7.38	1.5
80	6.73	7.86	1.5
90	7.15	8.32	1.5
100	7.53	8.75	1.5
110	7.89	9.15	1.5
40	6.07	7.29	2
50	6.72	7.98	2
60	7.34	8.65	2
70	7.92	9.29	2
80	8.48	9.89	2
90	9.00	10.47	2
100	9.48	11.01	2
110	9.94	11.52	2
40	8.39	10.09	3
50	9.29	11.04	3
60	10.15	11.96	3
70	10.96	12.84	3
80	11.72	13.68	3
90	12.44	14.48	3
100	13.11	15.23	3
110	13.74	15.93	3
40	10.57	12.70	4
50	11.70	13.90	4
60	12.78	15.06	4
70	13.80	16.17	4
80	14.76	17.23	4
90	15.66	18.23	4
100	16.51	19.17	4
110	17.30	20.05	4

C.4 Vapor Condensation on the Outside Surface of Tubes

The correlation for the heat transfer coefficient during vapor condensation outside the preheater/condenser tubes was developed by Henning and Wangnick (1995),

$$h = 0.725\,(k_\ell^3 \rho_\ell (\rho_\ell - \rho_v) g \lambda_v / \delta_o \mu \Delta T)^{0.25}\, C_1 C_2 \qquad (C.4)$$

with $C_1 = 1.23795 + 0.353808 N_1 - 0.0017035 N_1^2$,

$C_2 = 1 - 34.313 X_{nc} + 1226.8 X_{nc}^2 - 14923 X_{nc}^3$,

$N_1 = 0.564\sqrt{N_t}$, and $N_t = \dfrac{4M_f}{\pi \delta_i^2 \rho_f V_f}$

Variations in the heat transfer coefficient are shown in Table C.4 and Fig. C.4.

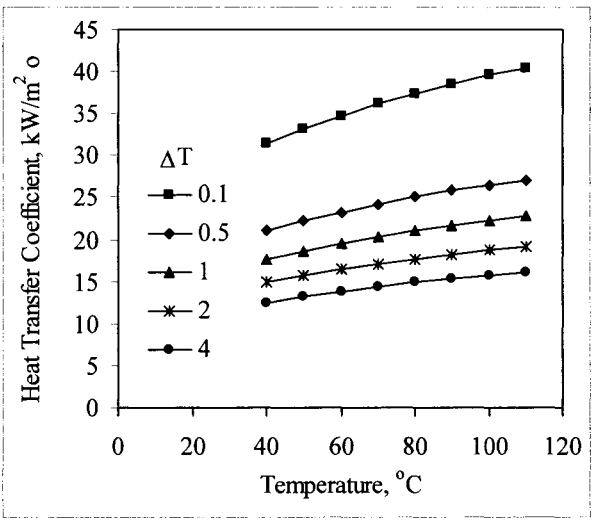

Fig. C.4. Variation in the heat transfer coefficient on the outside surface of tubes

Table C.4: Variation in the heat transfer coefficient during condensation on the outside surface of tubes. Parameters include $X_{nc} = 0.015$, $\delta_o = 0.03$ m, $M_f = 1$ kg/s, $V_f = 1.5$ m/s, $\delta_i = 0.025$ m. Calculated values include $N_t = 1.37$, $N_1 = 0.66$, $C_1 = 1.47$, $C_2 = 0.71$.

T (°C)	h (kW/m^2 °C)	ΔT (°C)	ρ_v (kg/m^3)	ρ_ℓ (kg/m^3)	k_ℓ (kW/m °C)	λ_v (kJ/kg)	μ_ℓ (kg/m s)
40	31.41	0.1	0.051	991.861	6.30E-04	2406.50	6.55E-04
50	33.12	0.1	0.083	987.683	6.41E-04	2382.52	5.48E-04
60	34.68	0.1	0.130	982.924	6.50E-04	2358.31	4.67E-04
70	36.11	0.1	0.198	977.602	6.58E-04	2333.76	4.04E-04
80	37.41	0.1	0.293	971.734	6.65E-04	2308.77	3.54E-04
90	38.56	0.1	0.424	965.339	6.71E-04	2283.25	3.14E-04
100	39.58	0.1	0.598	958.434	6.76E-04	2257.11	2.81E-04
110	40.47	0.1	0.826	951.037	6.79E-04	2230.25	2.54E-04
40	21.01	0.5	0.051	991.861	6.30E-04	2406.50	6.55E-04
50	22.15	0.5	0.083	987.683	6.41E-04	2382.52	5.48E-04
60	23.19	0.5	0.130	982.924	6.50E-04	2358.31	4.67E-04
70	24.15	0.5	0.198	977.602	6.58E-04	2333.76	4.04E-04
80	25.02	0.5	0.293	971.734	6.65E-04	2308.77	3.54E-04
90	25.79	0.5	0.424	965.339	6.71E-04	2283.25	3.14E-04
100	26.47	0.5	0.598	958.434	6.76E-04	2257.11	2.81E-04
110	27.07	0.5	0.826	951.037	6.79E-04	2230.25	2.54E-04
40	17.66	1	0.051	991.861	6.30E-04	2406.50	6.55E-04
50	18.62	1	0.083	987.683	6.41E-04	2382.52	5.48E-04
60	19.50	1	0.130	982.924	6.50E-04	2358.31	4.67E-04
70	20.31	1	0.198	977.602	6.58E-04	2333.76	4.04E-04
80	21.04	1	0.293	971.734	6.65E-04	2308.77	3.54E-04
90	21.69	1	0.424	965.339	6.71E-04	2283.25	3.14E-04
100	22.26	1	0.598	958.434	6.76E-04	2257.11	2.81E-04
110	22.76	1	0.826	951.037	6.79E-04	2230.25	2.54E-04
40	14.85	2	0.051	991.861	6.30E-04	2406.50	6.55E-04
50	15.66	2	0.083	987.683	6.41E-04	2382.52	5.48E-04
60	16.40	2	0.130	982.924	6.50E-04	2358.31	4.67E-04
70	17.08	2	0.198	977.602	6.58E-04	2333.76	4.04E-04
80	17.69	2	0.293	971.734	6.65E-04	2308.77	3.54E-04
90	18.24	2	0.424	965.339	6.71E-04	2283.25	3.14E-04
100	18.72	2	0.598	958.434	6.76E-04	2257.11	2.81E-04
110	19.14	2	0.826	951.037	6.79E-04	2230.25	2.54E-04
40	12.49	4	0.051	991.861	6.30E-04	2406.50	6.55E-04
50	13.17	4	0.083	987.683	6.41E-04	2382.52	5.48E-04
60	13.79	4	0.130	982.924	6.50E-04	2358.31	4.67E-04
70	14.36	4	0.198	977.602	6.58E-04	2333.76	4.04E-04
80	14.87	4	0.293	971.734	6.65E-04	2308.77	3.54E-04
90	15.33	4	0.424	965.339	6.71E-04	2283.25	3.14E-04
100	15.74	4	0.598	958.434	6.76E-04	2257.11	2.81E-04
110	16.09	4	0.826	951.037	6.79E-04	2230.25	2.54E-04

C.5 Water Flow in Plate Heat Exchanger

The heat transfer coefficient in plate heat exchangers is developed by Buonopane et al. (1974) and is given in terms of variations in the Nusselt number as a function of the Reynolds and Prandtl numbers of the fluid; this is

$$h = 0.2536\ Re^{0.65}\ Pr^{0.4}\ (k_w/De) \qquad (C.5)$$

Where Re is the Reynolds number, which is defined in terms of the effective diameter ($Re = De\ \rho\ v/\mu$), Pr is the Prandtl number, and De is the equivalent diameter, which is defined by $De = 4\ (wd)/(2(w+d))$. In the above equations, ρ is density, μ is viscosity, k is thermal conductivity, Cp is heat capacity, v is velocity, w is plate width, and d is plate spacing. Variations in the heat transfer coefficient are shown in Table C.5 and Fig. C.5 as a function of temperature and velocity. Values for physical properties, which includes μ, k, Cp, and ρ are given Table C.1.

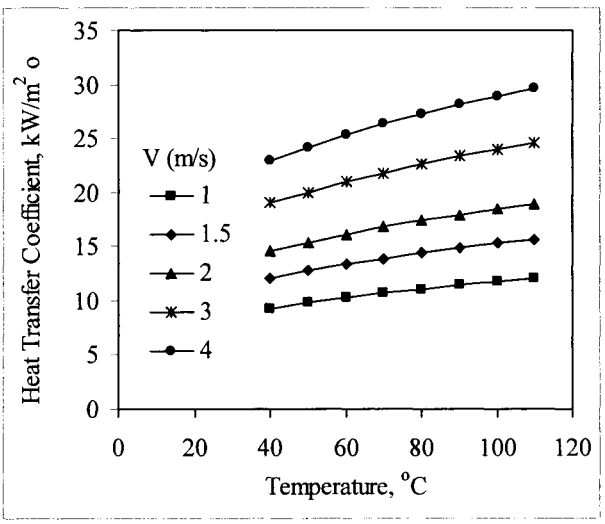

Fig. C.5. Variation in the heat transfer coefficient for seawater flowing in plate heat exchanger

Table C.5: The heat transfer coefficient in plate heat exchanger for w = 0.2 m, d = 0.02 m, De = 0.036 m, X = 40,000 ppm.

T (°C)	h (kW/m^2 °C)	V (m/s)	Re	Pr
40	9.31	1	51859.68	4.54
50	9.80	1	61515.64	3.75
60	10.26	1	71652.80	3.16
70	10.68	1	82165.87	2.71
80	11.07	1	92955.63	2.36
90	11.42	1	103930.25	2.08
100	11.75	1	115006.00	1.86
110	12.04	1	126107.45	1.68
40	12.11	1.5	77789.52	4.54
50	12.76	1.5	92273.46	3.75
60	13.35	1.5	107479.19	3.16
70	13.90	1.5	123248.80	2.71
80	14.41	1.5	139433.44	2.36
90	14.87	1.5	155895.38	2.08
100	15.29	1.5	172509.00	1.86
110	15.66	1.5	189161.18	1.68
40	14.60	2	103719.37	4.54
50	15.38	2	123031.28	3.75
60	16.10	2	143305.59	3.16
70	16.76	2	164331.73	2.71
80	17.37	2	185911.26	2.36
90	17.93	2	207860.50	2.08
100	18.43	2	230012.00	1.86
110	18.89	2	252214.91	1.68
40	19.01	3	155579.05	4.54
50	20.02	3	184546.93	3.75
60	20.96	3	214958.39	3.16
70	21.82	3	246497.60	2.71
80	22.61	3	278866.88	2.36
90	23.33	3	311790.76	2.08
100	23.99	3	345018.00	1.86
110	24.58	3	378322.36	1.68
40	22.91	4	207438.73	4.54
50	24.14	4	246062.57	3.75
60	25.26	4	286611.19	3.16
70	26.30	4	328663.46	2.71
80	27.26	4	371822.51	2.36
90	28.13	4	415721.01	2.08
100	28.92	4	460023.99	1.86
110	29.63	4	504429.82	1.68

C.6 Condensers and Evaporators Overall Heat Transfer Coefficient

Several correlations are available for the overall heat transfer coefficient. Predicted values by theses correlations vary between lows of 2 kW/m^2 °C up to highs of 4 kW/m^2 °C. Variations depend on the fouling resistance and the surface conditions. Results for these correlations are shown in Fig. C.6. The following is a list of these correlations:

- Fouled condenser, El-Dessouky et al. (1998)

$$U_c = 1x10^{-3} (1617.5 + 0.1537\ T + 0.1825\ T^2 - 0.00008026\ T^3) \quad (C.6)$$

- Fouled evaporator, El-Dessouky et al. (1998)

$$U_e = 1x10^{-3} (1939.4 + 1.40562\ T - 0.0207525\ T^2 + 0.0023186\ T^3) \quad (C.7)$$

- Fouled condenser, Takada et al. (1983)

$$U_c = 0.8\ (3 + 0.05\ (T - 60)) \quad (C.8)$$

- Clean drop wise condenser, Bromly et al. (1970)

$$U_c = 1x10^{-3} (5186 - 90.82\ T + 0.5566\ T^2 - 0.0009159\ T^3)/0.17612 \quad (C.9)$$

- Clean film wise condenser, Bromly et al. (1970)

$$U_c = 1x10^{-3} (-316.2 + 6.62\ T)/0.17612 \quad (C.10)$$

- Oxidized film wise condenser, Bromly et al. (1970)

$$U_c = 1x10^{-3} (-64.37 + 4.625\ T)/0.17612 \quad (C.11)$$

In the above equations, U_c is the condenser overall heat transfer coefficient (with vapor condensing on the outside surface and seawater flow on the tube side), U_e is the evaporator overall heat transfer coefficient (with water forming a falling film on a horizontal tube bundle and vapor is condensing inside the tubes), and T is the evaporation/condensation temperature. As is shown in Fig. C.6 the units of (U) and (T) are kW/m^2 °C and °C, respectively. It should be noted that Fig. C.6 includes additional data points by other investigator; however, these investigators did not provide a correlation. In addition, the clean overall heat

transfer coefficient by El-Dessouky et al. (1998) is the same as Eqs. (C.6) and C.7), where it uses a fouling resistance of 0.08 m^2 °C/kW.

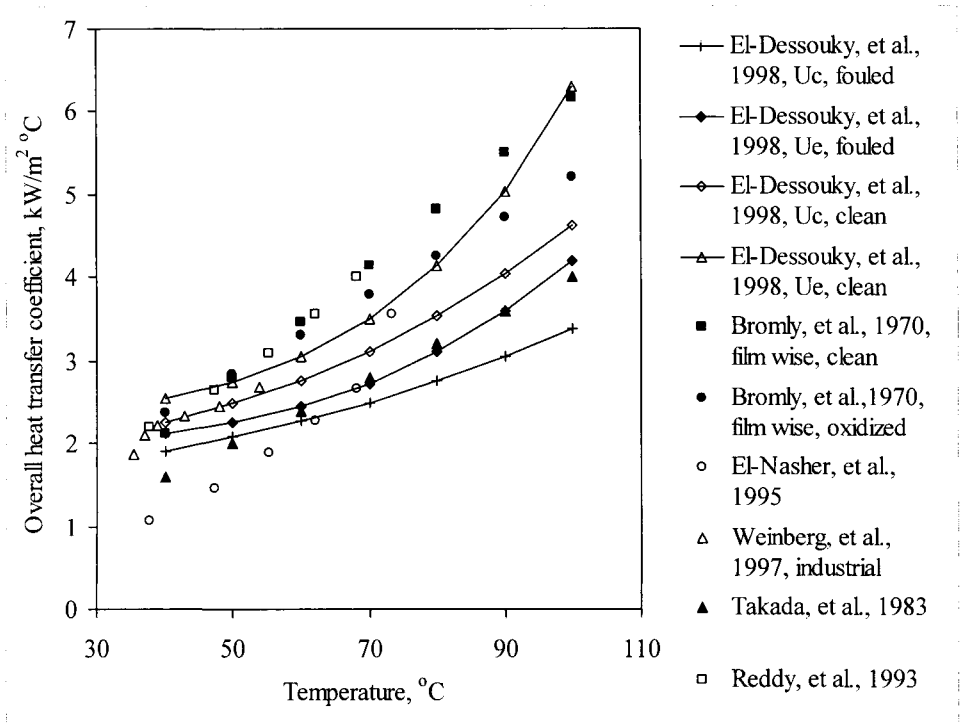

Figure 4: Variations in the overall heat transfer coefficient predicted by various correlations and as a function of temperature.

References

Bromley, L.A., and Read, S.M., Multiple effect flash (MEF) evaporator, Desalination, **70**(1970)3413-391.

Buonopane, R.A., Troupe, R.A., and Morgan, J.C., Heat transfer design method for plate heat exchangers, Chem. Eng. Progress, **59**(7)(1963)57-61.

El-Dessouky, H., Alatiqi, I., Bingulac, S., and Ettouney, H., Steady-state analysis of the multiple effect evaporation desalination process, Chem. Eng. Technol., **21**(1998)15-29.

El-Nashar, A.M., and Qamhiyeh, A.A., Simulation of the steady-stage operation of a mulit-effect stack seawater distillation plant, Desalination, **101**(1995)231-243.

Han, J. and Fletcher, L., Falling film evaporation and boiling in circumferential and axial grooves on horizontal tubes, Ind. Eng. Chem. Process Des. Dev., **24**(1985)570-597.

Henning, S, and Wangnick, K., Comparison of different equations for the calculation of heat transfer coefficients in MSF multi-stage flash evaporators, Proceedings of the IDA World Congress on Desalination and Water Sciences, Abu Dhabi, November, 1995, Vol. III, pp. 515-524.

Reddy, G.P., Husain, A., and Al-Gobaisi, D.M.K., Modelling and optimization of muliple effect horizontal tube falling film evaporators, Proceeding of the IDA World Congress on Desalination and Water Sciences, Madrid, Spain, October, 1997, Vol. I, pp 131-149.

Shah, M.M., Heat transfer, pressure drop, visual observations, test data for ammonia evaporating inside tubes, ASHRAE Trans., Vol. 84, Part 2, 1978.

Takada, M., and Drake, J.C., Application of improved high performance evaporator, Desalination, **45**(1983)3-12.

Wangnick, K., How incorrectly determined physical and constructional properties in the seawater and brine regimes influence the design and size of an MSF desalination plant - stimulus for further thoughts, Proceedings of the IDA World Congress on Desalination and Water Science, Abu Dhabi, November, 1995, Vol. II, pp. 201-218.

Weinberg, J., and Ophir, A., Ashdod experience and other dual purpose desalination plants based on multi effect desalination with aluminum tubes, Symposium on Desalination of Seawater with Nuclear Energy, Taejon, Republic of Korea, May, 1997.